MEASUREMENT OF SWITCHING TRANSITIONS IN IGBTS

Master Thesis
by

Francis Mulolani
Xiaoxiao Ni

Division of Electric Power Engineering
Department of Energy and Environment
CHALMERS UNIVERSITY OF TECHNOLOGY
Gothenburg, Sweden 2006

Abstract

In this project, an experimental set-up was designed and constructed for the purpose of measuring switching losses in IGBTs. As part of the set-up a high frequency current measuring transformer was also designed and constructed and its performance was compared to that of a commercial current measuring probe. From the voltage and current measurements switching losses were determined under different conditions. The switching losses were determined for a range of voltages and it was observed that they varied linearly with the voltage level at a constant value of current. The effect of changing the value of the gate resistance was also studied and it was found that increasing the gate resistance increased the switching losses. The turn-off losses were found to be significantly higher than the turn-on losses because the turn-off transition was done at a higher current level than the turn-on transition. It was also found that increasing the temperature of the IGBT module increased the losses.

Key words: IGBT, switching losses, transition, turn-on, turn-off, measurements

Preface

This thesis work was carried out at the Division of Electric Power Engineering, Department of Energy and Environment of Chalmers University of Technology as part of the International Masters Programme in Electric Power Engineering. It provided a good opportunity to learn more about the switching behaviour of IGBTs and practical measurements at high frequencies.

The authors would like to thank the following people who contributed to make the work a success. Their supervisor and examiner Prof. Torbjörn Thiringer for coming up with the idea of the project and for continuous advice, encouragement and support during its course; Dr. Jörgen Blennow for advice during the construction; Robert Karlsson for advice and help with the circuits; Magnus Ellsén for help in the workshop; Torsten Nilson for advice on the design of the CT; their fellow masters students and other staff at the department; family and friends for their love and support.

TABLE OF CONTENTS

1.0 INTRODUCTION

1.1 Background

The IGBT is a relatively new power semi-conductor device which was developed in the early 1980s due to a need to combine the desirable characteristics of the bipolar junction transistor (BJT) and the MOSFET. MOSFETS can be turned on and off much faster, but have large on-state losses especially at voltages exceeding 200V while BJTs have lower conduction losses but have longer switching times [2]. BJTS are current controlled devices and require a complex base drive circuit while MOSFETs are voltage controlled devices requiring simpler gate drive circuits.

This led to the development of the IGBT which is a device whose performance is a compromise between a MOSFET and a BJT. It is faster than a BJT but slower than a MOSFET, and its on-state losses are lower than those of a MOSFET but comparable to a BJT. It has a MOS gate input structure which has a simple gate control circuit design and is capable of fast switching up to 100kHz [2]. Its output has a bipolar transistor structure which gives it a good current conduction capability.

Its high forward conduction current density and very low on-state voltage drop are due to conductivity modulation. Because of the high current density a smaller chip size is possible and the cost can be reduced. It has a low driving power and a simple drive circuit due to the input MOS gate structure, thus, the IGBT can easily be controlled as compared to current controlled devices (thyristor, BJT) in high voltage and high current applications. With respect to output characteristics, the IGBT has superior current conduction capability compared with the bipolar transistor. It also has excellent forward and reverse blocking capabilities. This gives it a wider SOA (Safe Operating Area).

However, on the negative side, its switching speed (less than 100 kHz) is inferior to that of the power MOSFETs, but it is superior to that of the BJT. The collector current tailing due to the minority carrier causes the turn-off speed to be slow. Tailing current will be discussed further in Chapter 2. There is also the possibility of latch-up due to the internal PNPN thyristor structure [3]. This will also be discussed further in Chapter 2.

While the first commercially available IGBTs did not exceed blocking voltages up to 600V, and currents of a few amperes, development started aimed at increasing the power handling capability continually. Currently, high voltage IGBT chip sets rated up to 6.5kV are successfully manufactured for 3.6kV DC link applications. This trend is fuelled by a growing number of new applications in the fields of traction systems, industrial applications and HVDC converters [4].

Thus, it is necessary to have a reliable method of determining the expected power losses in the device for different applications. The most reliable method is by experimental testing.

1.2 Aim

The aim of the project is to design and build an experimental set-up for the investigation of turn-on and turn-off transitions of high voltage IGBTs; and from these measurements to determine the energy losses per switching transition at turn-on and turn-off under different conditions and draw a conclusion of the factors affecting the switching losses.

1.3 Thesis Layout

Chapter 2 will review the theory of the IGBT covering its physical and constructional structure, switching characteristics and calculation of switching losses.

Chapter 3 describes the experimental test setup and gives an overview of the circuits used for the tests.

Chapter 4 describes the measurement setup, the selection of the measurement techniques and construction of a current transformer to measure the transient current.

Chapter 5 describes the experimental results and their analysis. Effects of varying the test conditions are also discussed.

Chapter 6 gives the conclusion and recommendations for future work.

2.0 THEORY

This chapter discusses the theory of the IGBT regarding its structure, switching characteristics, and theoretical determination of the switching losses.

2.1 Structure

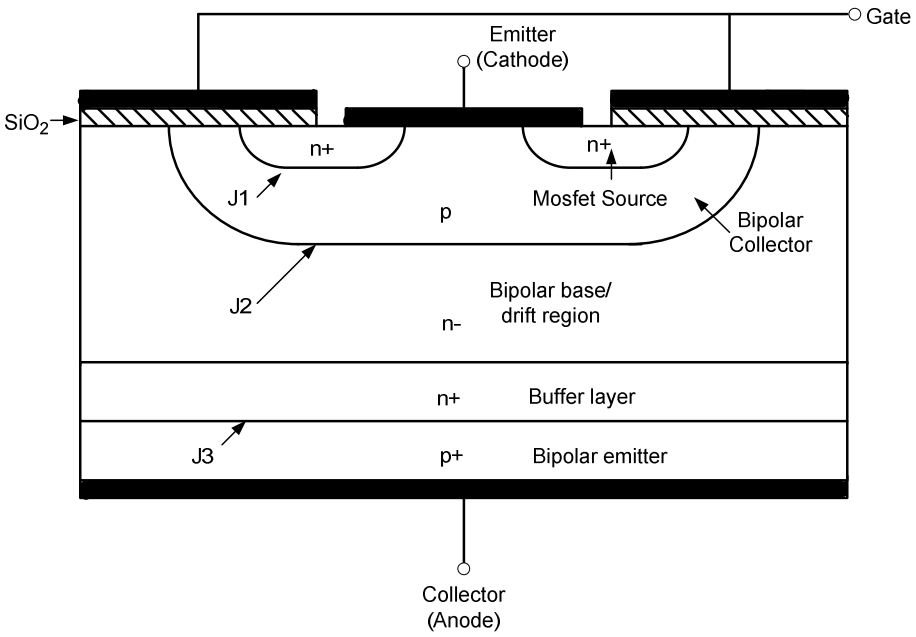

Fig 2.1 Typical IGBT Structure

Fig 2.1 shows the structure of a typical n-channel IGBT. This structure is very similar to that of a vertically diffused MOSFET featuring a double diffusion of a p-type region and an n-type region. By applying a suitable voltage to the gate, an inversion layer (same as in a MOSFET) will be formed under the gate and the IGBT will be turned on. The main difference is the use of a p+ substrate layer for the drain (collector). The effect of this is to change it into a bipolar device as this p-type region injects holes into the n-type drift region.

The input has a MOS gate structure, and the output is a wide base PNP transistor. Besides the PNP transistor, there is an NPN transistor, which is designed to be inactivated by shorting the base and the emitter to the MOSFET source metal. The 4 layers of PNPN, which comprises the PNP transistor and the NPN transistor, form a thyristor structure, which causes the possibility of a latch-up. This is the undesirable turn-on of this parasitic thyristor; and there are several structural modifications to the basic one shown in fig 2.1 to prevent this. Unlike the power MOSFET, it does not have an integral reverse diode that exists parasitically, and because of this it needs to be connected with the appropriate fast recovery diode when needed.

Fig 2.2 (a) shows the equivalent circuit of the IGBT showing the two transistors which make up the parasitic thyristor and the resistances of its regions. Fig 2.2(b) shows its symbol.

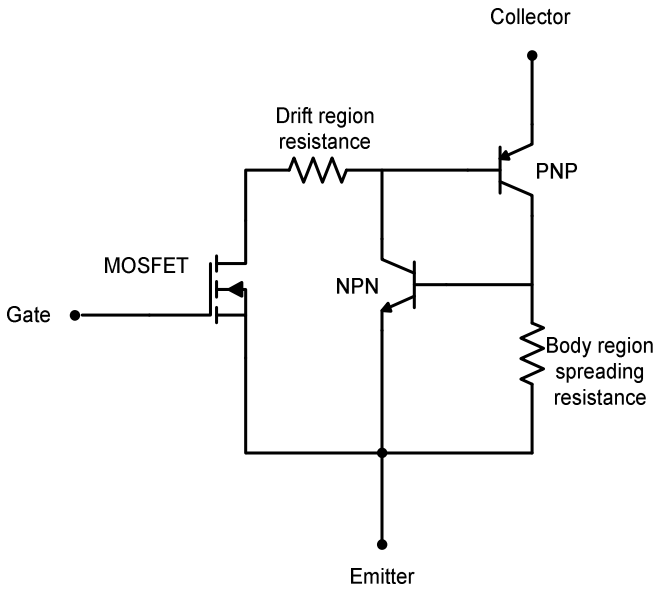

(a) IGBT equivalent circuit

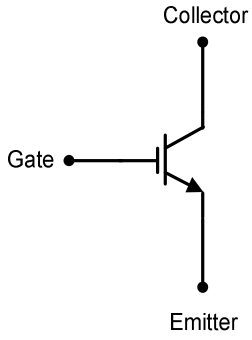

(b) IGBT Symbol

Fig 2.2 IGBT equivalent circuit and symbol

2.2.1 Punch-through and Non-punch-through

An IGBT is called a PT (punch-through) or asymmetrical when it has an n+ buffer layer between the p+ substrate and n- drift region (like the one shown in fig 2.1). If not, it is called an NPT (non-punch-through) IGBT or symmetrical IGBT. The n+ buffer layer improves turn-off speed by reducing the minority carrier injection quantity and by raising

the recombination rate during the switching transition. It also improves latch-up characteristics by reducing the current gain of the PNP transistor, though it causes the on-state voltage drop to increase. To get round this problem the n- drift region can be reduced with the result being the same forward blocking voltage because the n+ buffer layer improves the forward blocking capability. This gives PT-IGBTs an advantage over NPT-IGBTs as regards switching speed and forward voltage drop. However PT-IGBTs have lower reverse-blocking voltage capability due to the presence of the heavy doping regions on both sides of junction J_3 in fig 2.1.

2.1.2 I-V Characteristics

Fig 2.3(a) shows the output characteristics of an IGBT. These closely resemble those of a logic level BJT. However unlike the BJT where the controlling parameter is the base current, here the controlling parameter is the gate-emitter voltage (v_{GE}).

Fig 2.3(b) shows the transfer characteristic (v_{GE} vs. i_C) for the IGBT. It is identical to that for the MOSFET. If v_{GE} is less than the threshold voltage $V_{GE\,(th)}$, the IGBT is in the off state, and when it is greater than the threshold voltage then the IGBT goes into the on state. The maximum value of V_{GE} is usually limited by the maximum allowable value of I_C.

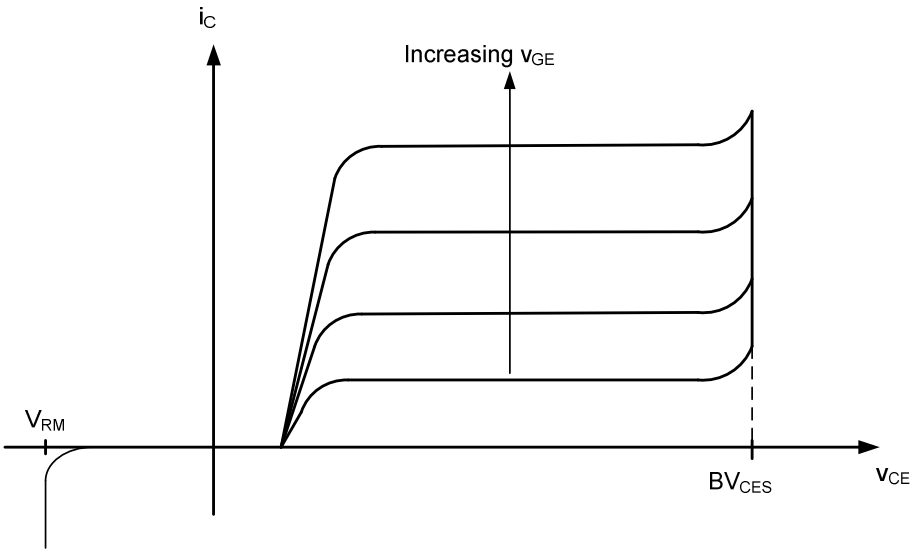

(a) IGBT output characteristics

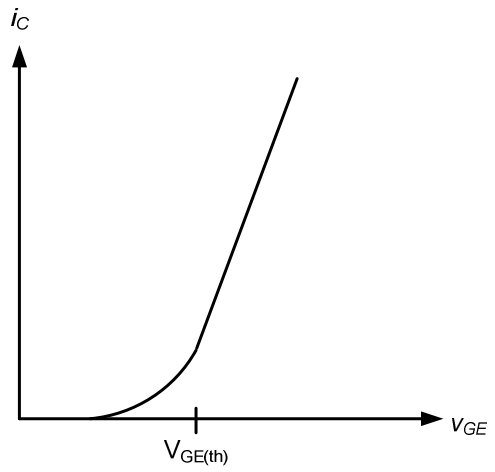

(b) IGBT transfer characteristics

Fig 2.3 IGBT characteristics

2.2 Operation

The operation of the IGBT can be divided into blocking-state and on-state. Below are discussed its behaviour in these two states.

2.21 Blocking State

In the blocking state, v_{GE} is less that $V_{GE\,(th)}$ and the IGBT is off. This is because there is no MOSFET inversion layer formed in this state. Only a small leakage current can flow in this state and all the applied forward voltage falls across the reverse biased junction J2 (see fig 2.1) which is between the p body region and the n- drift region. The forward breakdown voltage is therefore determined by the breakdown voltage of this junction, which also depends on the doping level of the n- drift region. The lower doping results in a wider depletion region and hence a lower maximum electric field within this region. To prevent the depletion region from extending into the p+ collector region, the n+ buffer layer is added. However, as stated above this reduces the reverse breakdown voltage, but it allows the drift region to be reduced, thus reducing on-state losses.

2.2.2 On-State

Increasing v_{GE} beyond $V_{GE\,(th)}$ turns on the IGBT. This causes an inversion layer to form under the gate providing a channel linking the emitter to the drift region. Electrons are then injected from the emitter into the n- drift region while holes are injected into the drift region from the p+ collector region. This is illustrated in fig 2.4.

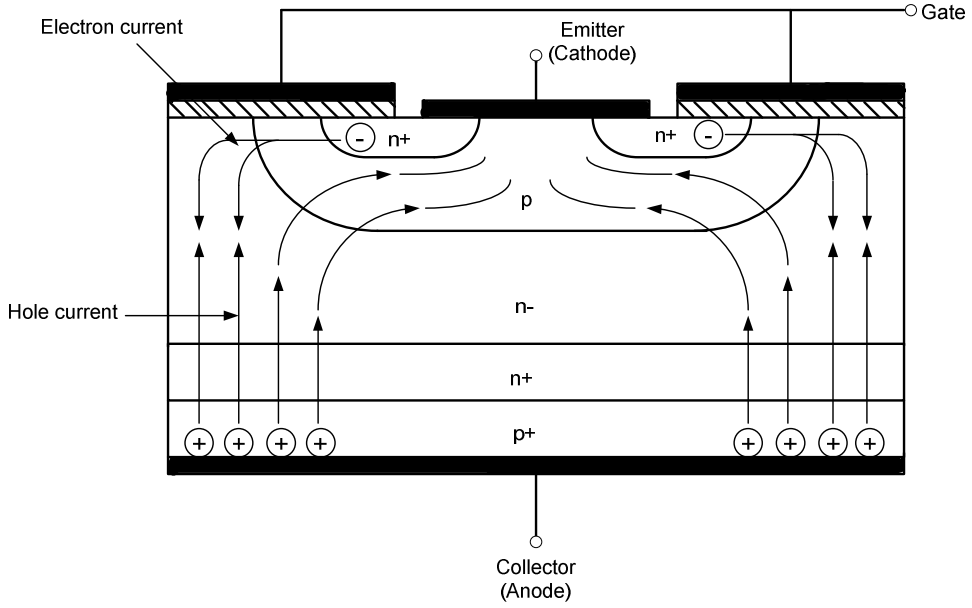

Fig 2.4 Hole current and electron current flow in the IGBT during on-state

This injection of charges causes conductivity modulation of the drift region where the electron and hole densities are much higher than the original n- doping level. Conductivity modulation gives the IGBT its low on-state voltage drop due to the reduced resistance of the drift region. Some of the injected holes recombine in the drift region, while others reach the junction with the p-type region where they are collected. It is from this behaviour that the equivalent circuit for the IGBT shown in fig 2.2(a) is derived.

2.3 Latch-up

As stated earlier, the IGBT has a parasitic thyristor due to the PNPN structure between the collector and the emitter. Latch-up means the turning on of this thyristor. If this happens the IGBT current is no longer controlled by the MOS gate, and the IGBT would be destroyed due to excessive power dissipation produced caused by this current. In this instance the only way to turn off the IGBT will be by forced commutation, like a conventional thyristor.

Latch-up is caused in two ways namely static latch-up and dynamic latch-up.

2.3.1 Static latch-up

Electrons are injected into the drift region under the gate electrode and increase its conductivity, while most of the holes injected into the drift region are injected at the p body region and flow laterally to the emitter along the bottom of the n+ emitter region. This causes a lateral voltage drop in the ohmic resistance of the p body region (body region spreading resistance in fig 2.2(a)). If this voltage drop becomes greater than the potential barrier of the n+ emitter/p body layer junction (J1 in fig 2.1), electrons are injected from the emitter to the p body layer and the NPN transistor formed by the n+ emitter, p body and n- drift region is turned on. If the sum of the two transistors' current gains becomes 1 ($\alpha_{NPN}+\alpha_{PNP}\geq 1$) the PNP transistor will turn on as well and hence the parasitic thyristor made up of these transistors will latch on and latch-up of the IGBT will have occurred.

2.3.2 Dynamic latch-up

This occurs when the IGBT is being switched from on to off and it occurs at current values much lower than for static latch-up. It is caused by the abrupt extension of the depletion layer of the n+ drift/p body junction (J2 in fig 2.1) due to the rapid build-up of collector-emitter voltage which must be supported across this junction. This increases α_{PNP} and a greater fraction of holes injected into the drift region is collected by the junction J2 in fig 2.1. This increases the lateral hole current magnitude and hence the lateral voltage drop, thus satisfying the conditions for latch-up.

Latch-up is undesirable and should be avoided. One way of avoiding it is by preventing the turn on of the NPN transistor, and another way is to keep the sum of the two transistors' current gains less than 1($\alpha_{NPN}+\alpha_{PNP}<1$). The user should also ensure that the IGBT is used in circuits where the possibility of overcurrents exceeding I_{CM} is minimized. There are also many structural modifications which different manufacturers use to avoid latch-up.

2.4 Switching Characteristics

2.4.1 Turn-on

Fig 2.5 shows the typical turn-on waveforms of the IGBT. v_{GE} (t) is the gate drive voltage. At the beginning of the time $t_{d(on)}$, the signal to turn on the IGBT is received from the control circuit and the gate drive voltage starts to increase at a rate determined by the value of the gate input capacitance ($C_{ies} = C_{ge} + C_{gc}$). When it reaches the value of the gate threshold voltage $V_{GE\ (th)}$, at the end of $t_{d\ (on)}$, the gate drive voltage stays constant, and the collector current starts to increase from zero to maximum. The time taken for the collector current to reach its maximum value of I_L is the current rise time t_{ri}. Meanwhile the collector-emitter voltage is falling in two stages. At the instant the current reaches I_L, the voltage starts to fall at a rate determined by the input capacitance at the gate. This is the time interval t_{fv}. The gate input capacitance is voltage dependent, and as the voltage decreases it increases and the rate of fall of the voltage decreases towards the end of the interval t_{fv}. At the end of this interval, the IGBT is fully on, and it is carrying the full load current I_L, and only a small voltage appears across it given by $V_{CE(on)}$. The gate drive voltage v_{GE}(t) then continues increasing at a slower rate than before due to the increased value of the gate input capacitance until it reaches V_{GG+}, the maximum applied voltage to the gate.

2.4.2 Turn-off

Turn-off of the IGBT is achieved by shorting the gate to the emitter or applying a negative voltage to the gate. Applying a negative voltage has the advantage of speeding up the turn-off process. The turn-off process is basically a reverse of the turn-on process. Fig 2.6 shows that the collector current falls in two stages. The first stage starts when the electron current supplied through the MOSFET channel during the on-state is stopped. The collector current falls abruptly in the time interval t_{fi1}. The remaining current falls at a slower rate during the time interval t_{fi2}. This is called the tail current and it comes from the minority carriers (holes) injected through the N- drift region from the P+ substrate during the on-state.

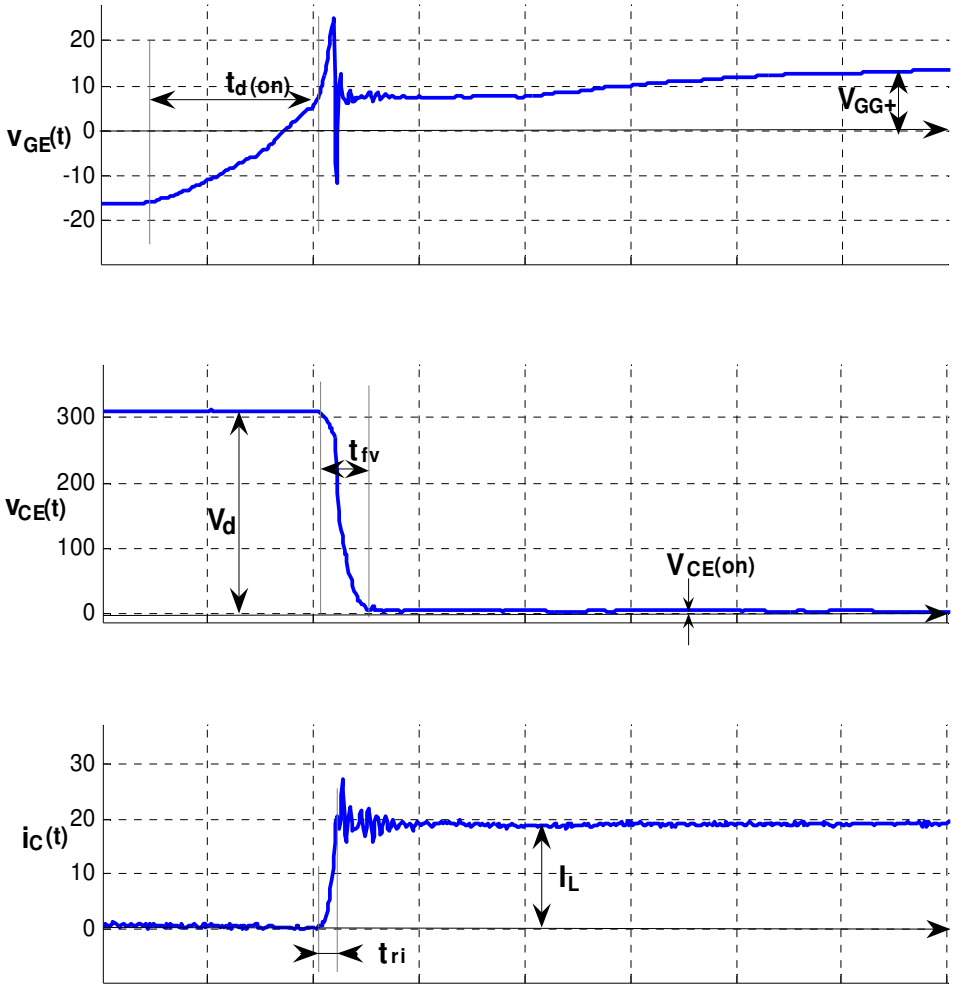

Fig 2.5 Measured IGBT turn-on waveforms

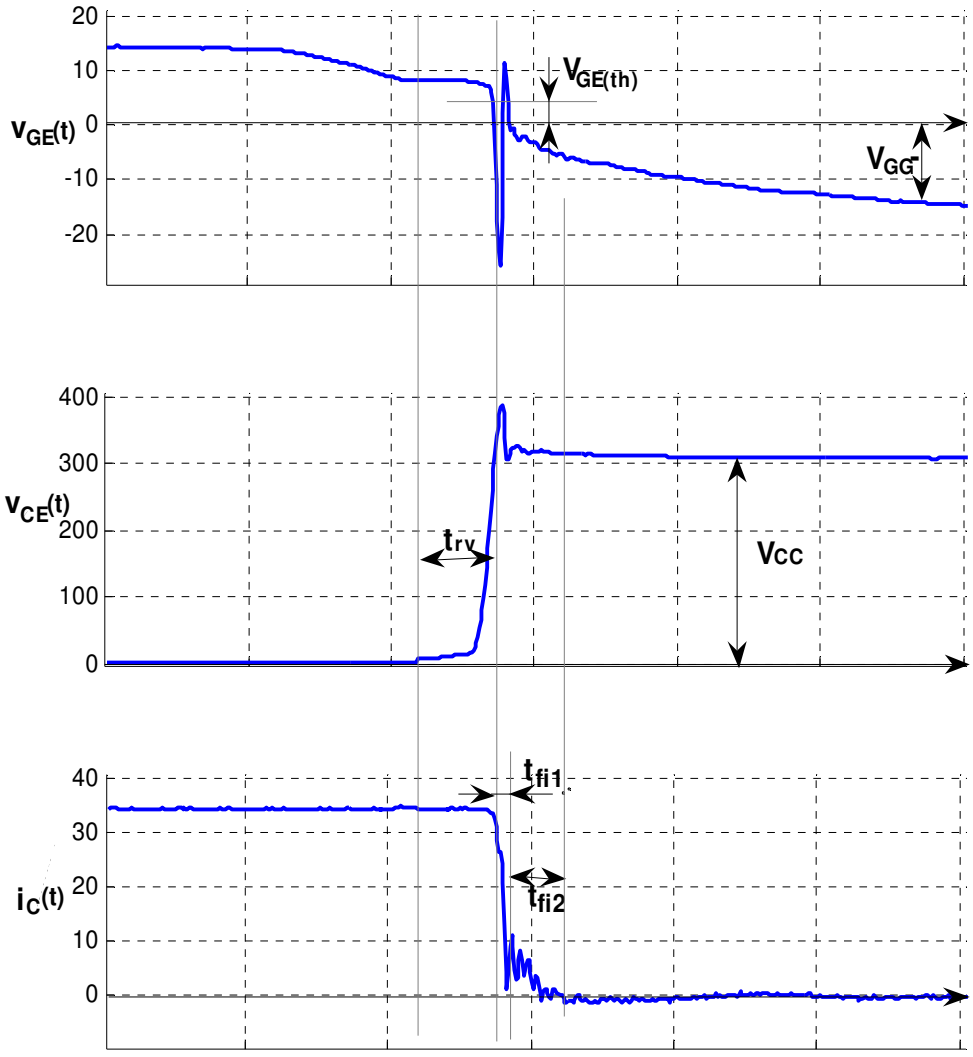

Fig 2.6 Measured IGBT turn-off waveforms

2.5 Calculation of Switching Energy Losses

Fig 2.7 shows typical waveforms which can be used to determine the switching losses of the IGBT in a diode clamped inductive load circuit. The switching losses can be divided into two parts, the turn-on losses and the turn-off losses.

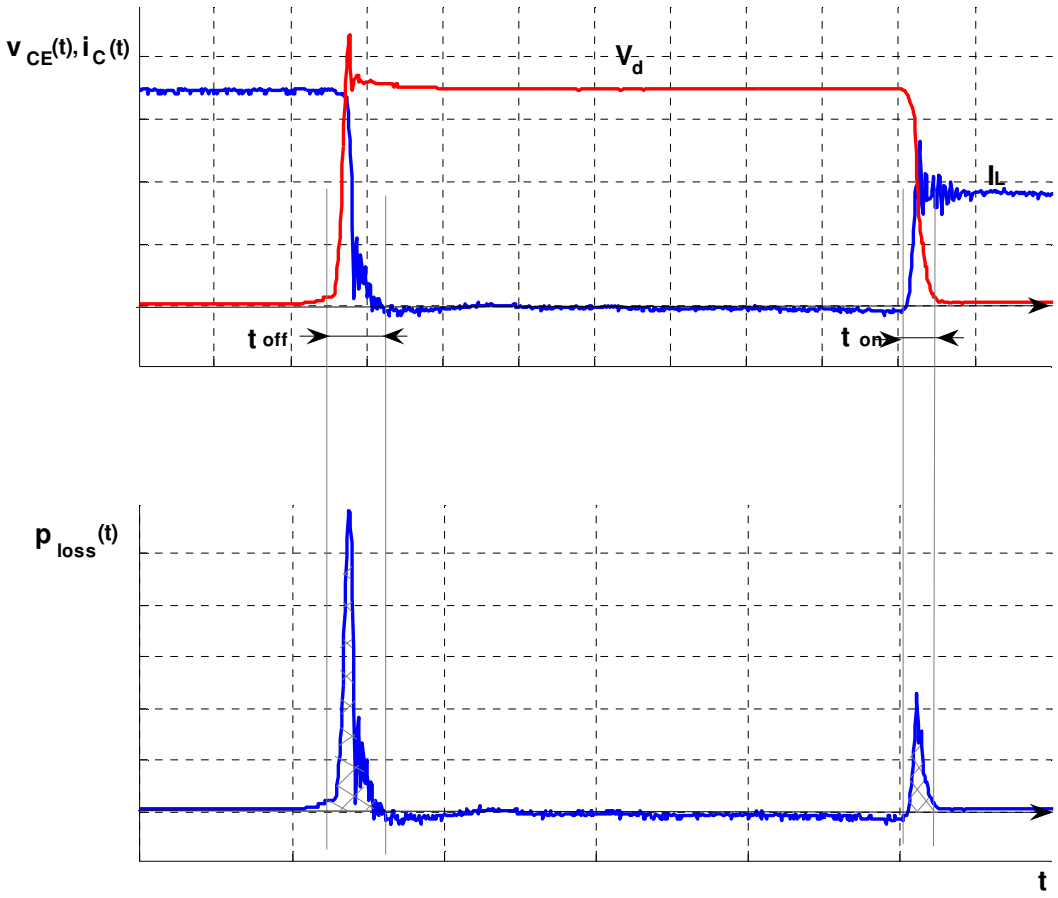

Fig 2.7 Measured IGBT waveforms for determining switching losses

2.5.1 Energy Loss at Turn-on

This is the amount of total energy lost during turn-on under inductive load, and it includes the loss from the diode reverse recovery. In practice, it is measured from the point where the collector current begins to rise to the point where the collector-emitter voltage falls to zero [2]. The power dissipated is given by

$$p_{loss\,(on)} = v_{CE}\,(t) i_C\,(t)\,. \tag{2-1}$$

The energy loss during this interval is calculated by finding the area under the power triangle as given by the equation below.

$$E_{loss(on)} = \int_{t_i}^{t_i + t_{on}} p_{loss(on)}\, dt\,. \tag{2-2}$$

Where t_i is chosen as the time when the current starts to rise and,
t_{on} is the total time for the turn-on transient.

2.5.2 Energy Loss at Turn-off

This is the amount of total energy lost during turn-off under inductive load. It is measured from the point where the collector-emitter voltage begins to rise from zero to the point where the collector falls completely to zero [2]. The power dissipated is given by

$$p_{loss(off)} = v_{CE}(t) i_C(t) . \tag{2-3}$$

The energy lost during this interval is given by

$$E_{loss(off)} = \int_{t_v}^{t_v + t_{off}} p_{loss(off)} dt . \tag{2-4}$$

Where t_v is the time when the voltage starts to rise, and
t_{off} is the total time for the turn off transient.

The total switching losses are calculated as the sum of $E_{loss\ (on)}$ and $E_{loss\ (off)}$.

3.0 EXPERIMENTAL SET-UP

An experimental set-up was designed and constructed to test IGBTs. The main parts of the set-up are the control circuit which generates the electronic signal to turn the IGBT on and off; the drive circuit which provides the required voltage and current level to turn the IGBT on and provide isolation between the logic level electronics and the main power circuit. The main power circuit consists of the IGBT module and other components at high voltage and high current.

3.1 Control Circuit

The control circuit determines when the IGBT is turned on and off. Thus it should generate a pulse or a series of pulses to turn the IGBT on and off.

The control circuit was designed to give two pulses, with a short delay time between them. The first pulse will turn the IGBT on and the current through the inductor will increase until it reaches a steady value. The IGBT is then turned off at the end of the first pulse and the current commutates to the diode. The diode conducts during the time delay between the two pulses. The second pulse turns the IGBT on again. Since the main interest is in the switching transients, (in the presence of both voltage and current) the first turn-off and the second turn-on are the points of interest.

The output of the control circuit goes to a fiber optic transmitter TOTX173, which is connected through a fiber optic connector HC 302-200 to a fiber optic receiver TORX173 which is at the input of the gate drive circuit. The fiber optic link provides isolation between the signal level electronics of the control circuit and the higher voltage levels present at the gate drive circuit. Moreover, the drive circuit shares the same grounding as the main power circuit, thus, there is need for signal isolation. Isolation can also be achieved using a signal HF transformer, or an opto-coupler. Fiber optics are the preferred choice because they have the advantage of providing higher electrical isolation, increased creepage distance and prevents retriggering of the IGBT at turn-on and turn-off due to the jump in the potential between the power device emitter reference point and the ground of the control electronics.

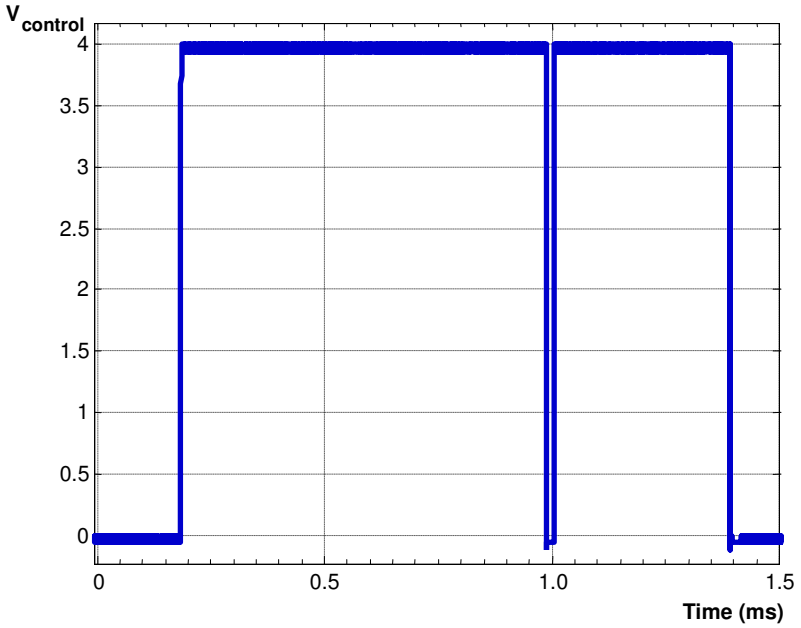

Fig 3.1 Control circuit output

3.2 Gate Drive Circuit

The gate drive circuit provides isolation between the control circuit and the main power circuit which is at a much higher potential and also provides the power required to turn the IGBT on and off. The IGBT is a voltage controlled device but during turn on, it draws current as the input capacitance C_{ies} is charged. Thus the drive circuit should be able to handle this current. To turn the IGBT on a voltage of 15V is applied to the gate, and to turn it off a voltage of -15V is applied. This is called bipolar voltage switching and it helps to make the turn off process faster than unipolar voltage switching, where zero voltage is applied at turn off.

Fig 3.2 shows the output stage of the drive circuit.

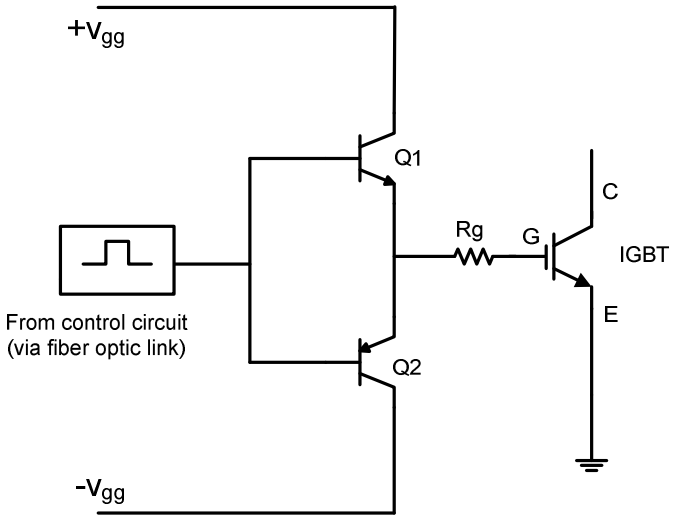

Fig 3.2 Output stage of gate drive circuit

When a signal comes from the control circuit to turn the IGBT on, transistor Q_1 is turned on and the voltage at the IGBT gate, V_{GE}, rises to 15V, and the IGBT is turned on. When the control signal goes to zero, transistor Q_2 is turned on and V_{GE} becomes -15V. The gate resistances R_g controls the rate of turn on or turn off of the IGBT (i.e. due to the charging and discharging of the gate capacitances respectively).

3.3 Main Test Circuit

Fig 3.3 shows the equivalent circuit of the experimental circuit.

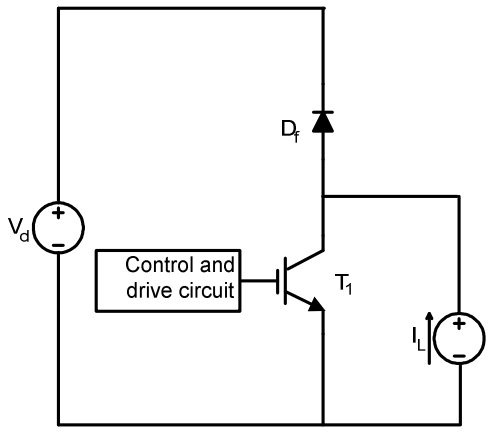

(a) Equivalent circuit

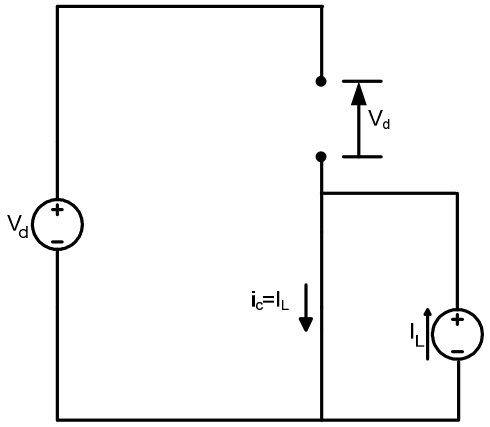

(b) IGBT conducting

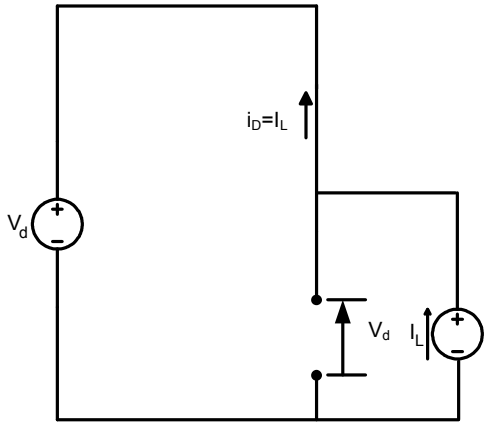

(c) Diode conducting

Fig 3.3 Equivalent circuit of test circuit

Fig 3.3 shows the equivalent circuit of the experimental set-up. V_d represents a stiff voltage while I_L represents a stiff current. Fig 3.3(b) shows the equivalent circuit when the IGBT is turned on and is conducting. The voltage V_d appears across the freewheeling diode D_f, and the current I_L flows through the IGBT. The IGBT is then turned off and the current commutates from the IGBT to the diode. Fig 3.3(c) shows the equivalent circuit when the diode is fully conducting and the IGBT is fully off. The voltage V_d then appears across the IGBT and the current I_L flows through the diode.

However during the commutation of current from the IGBT to the diode, there will be a time when there is both a voltage across and a current through the IGBT. This causes losses in the IGBT, and since they occur at its turn off they are called turn-off losses.

With the diode conducting the IGBT is turned on again, and the current commutates from the diode to the IGBT. Again there is an interval when the IGBT has to withstand a voltage across it and current through it at the same time and there will be losses during this interval. These losses are called the turn-on losses.

Together the turn-on and turn-off losses make up the switching losses which are a major part of the total losses in the IGBT.

Fig 3.4 shows the actual circuit implemented in the test set-up.

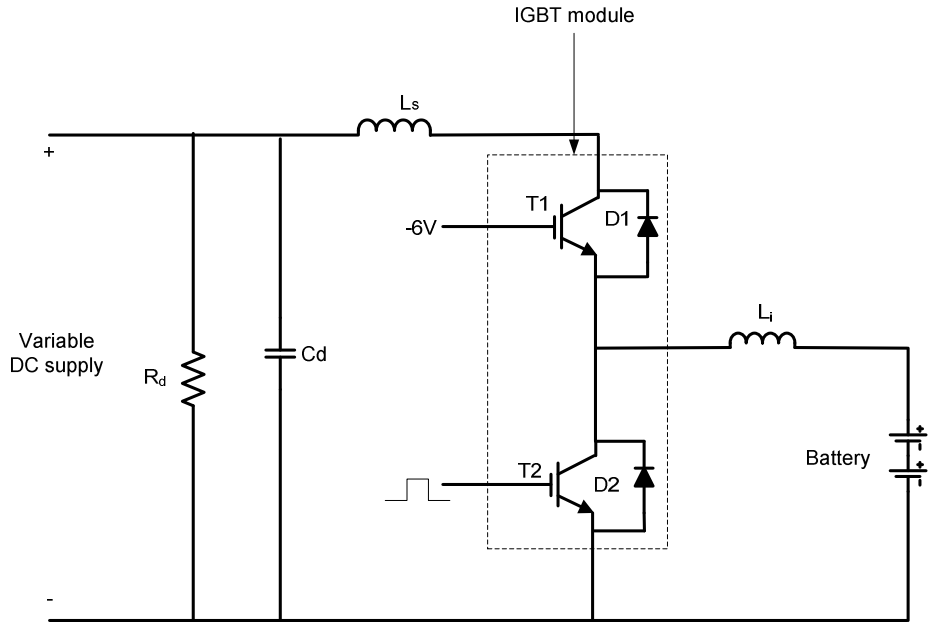

(a) Schematic of test set-up

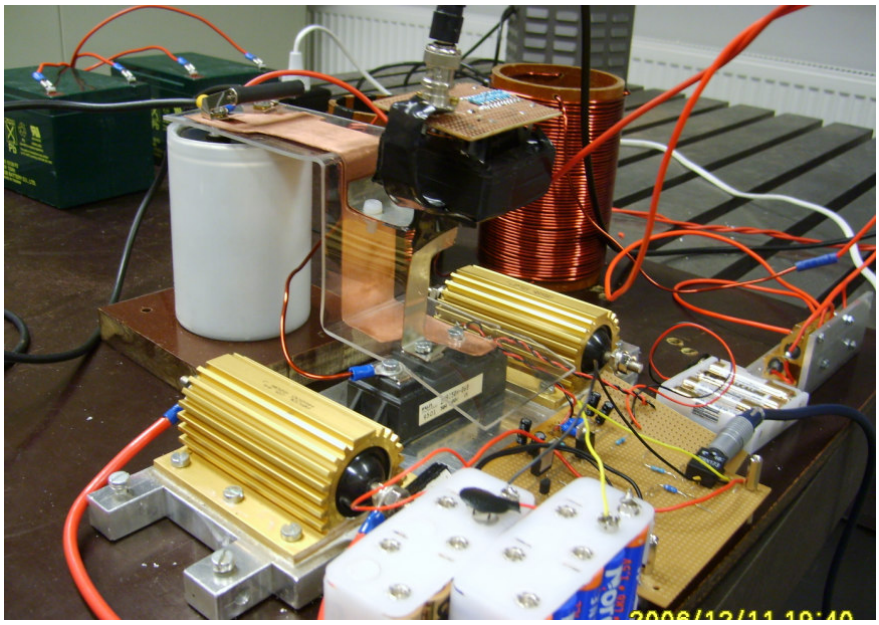

(b) Picture of test set-up

Fig 3.4 Diode Clamped Inductive Load Test Circuit

The variable DC voltage source and the capacitor C_d closely approximate the stiff voltage source V_d. The 12V DC supply and the inductor L_i closely approximate the stiff current source I_L. The 12V supply charges the inductor to a desired current level determined by the size of the inductor and the duration of the first pulse width, when the IGBT is on, and the inductor discharges its stored energy through the diode when the IGBT is off. The IGBT module is a half-bridge module with inbuilt freewheeling diodes. Therefore, during testing, only one IGBT need to be turned on and off, while the other one is kept off by applying a negative voltage to its gate.

3.4 Inductor Design

The inductor L_i was designed and constructed in this thesis work. The universal formula given by Equation (3-1) below, which is valid for an air-core(coreless) circular coil, was used for the design [5].

$$L = \frac{d^2 N^2}{18d + 40l} \quad . \tag{3-1}$$

Where L is the inductance in microhenry;
d is the coil outer diameter in inches;
N is the number of turns of the coil;
l is the coil length in inches.

A relatively low value of inductance is desirable so that the time taken for the current to rise to the required level is minimized. A value of 150μH was chosen, and by solving (3-1) numerically suitable values of d, l and N were determined as d=90mm, l=120mm and N=55. Fig 3.5(a) shows a picture of the inductor and fig 3.5(b) shows a cross sectional view with its dimensions.

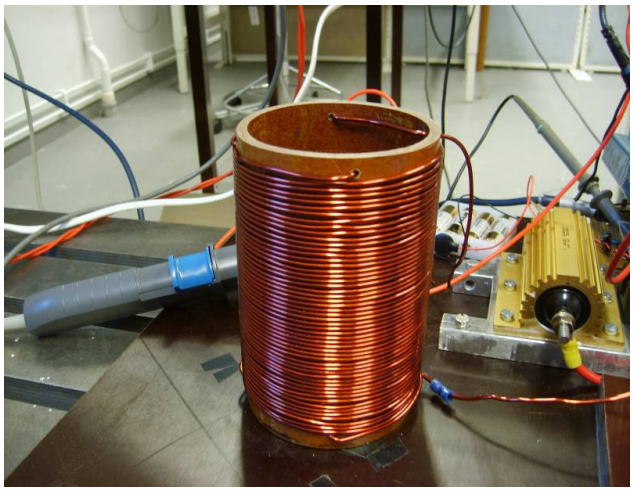

(a)Picture of the inductor

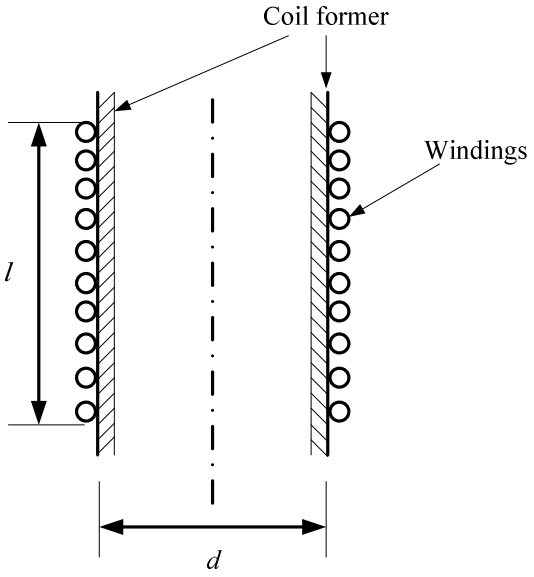

(b) Vertical cross section of the inductor showing dimensions

Fig 3.5 Photo and cross-sectional view of inductor

To determine the value of the inductor, the voltage across the inductor in the circuit of fig 3.4 was measured, and the rate of rise of current was also measured.

$$L = \frac{V_L}{di/dt}. \tag{3-2}$$

Where V_L is the voltage across the inductor, and

di/dt is the rate of rise of current.

The measured value of the inductor was found to be 160μH.

3.5 Heating Set-up

For the purpose of carrying out measurements at different temperatures, a set-up to increase the temperature of the IGBT module by external heating was included as part of the main experimental set-up. This included two 220Ω, 220W power resistors mounted on the same aluminium plate as the IGBT module and connected in parallel to the mains voltage through an auto-transformer. The heat dissipated by the power resistors to the

aluminium plate was conducted to the junction of the IGBT as shown by the thermal equivalent circuit below.

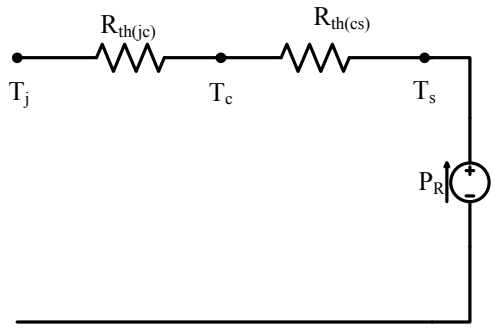

Fig 3.6 Thermal equivalent circuit of set-up (with heating resistors)

The temperature on the aluminium plate T_s was measured and the temperature of the IGBT junction T_j was then calculated using

$$T_j = T_s - P_R.(R_{th(jc)} + R_{th(cs)}) . \qquad (3\text{-}3)$$

Where T_j is the temperature of the junction
T_s is the temperature of the sink (aluminium plate)
P_R is the fraction of the power dissipated by the power resistors which goes to heat the sink
$R_{th(jc)}$ is the thermal resistance from junction to case
$R_{th(cs)}$ is the thermal resistance from case to sink

For the IGBT module under test, the thermal resistances are:
$R_{th(jc)}$ = 0.5˚C/W and $R_{th(cs)}$ = 0.05˚C/W (with thermal compound).

Fig 3.7 shows a picture of the heating resistors and the IGBT mounted on the aluminium plate.

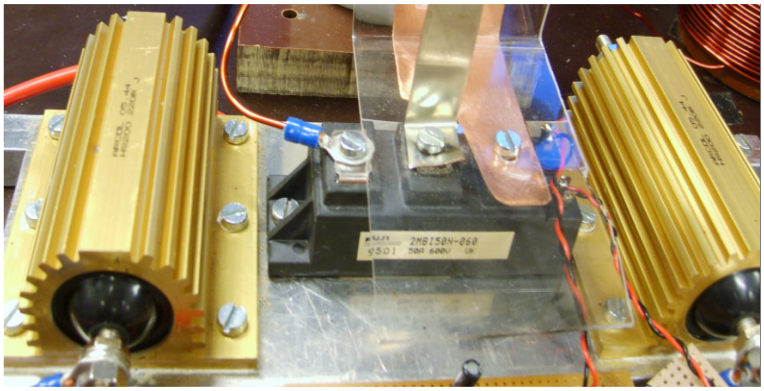

Fig 3.7 Picture of heating set-up

Since most of the power dissipated by the resistors will be lost in the form of radiation, convection and other means, only a small fraction will go to heat the aluminium plate, and, therefore, to simplify calculations it will be assumed that the surface temperature of the plate is equal to the junction temperature of the IGBT.

3.6 Simulation Setup

The test circuit was set-up in the simulation program OrCAD 10.5 as shown in fig 3.8. The IGBT and the diode were represented by the models from OrCAD, Z1MBI50L-060 and D1A BYT231PIV-400 respectively. Ls1 and Ls2 represent the estimated stray inductances. The other components were selected as similar as possible to the ones in the practical set-up. Simulations were carried out under the same conditions as the practical experiments and the results compared in Chapter 5.

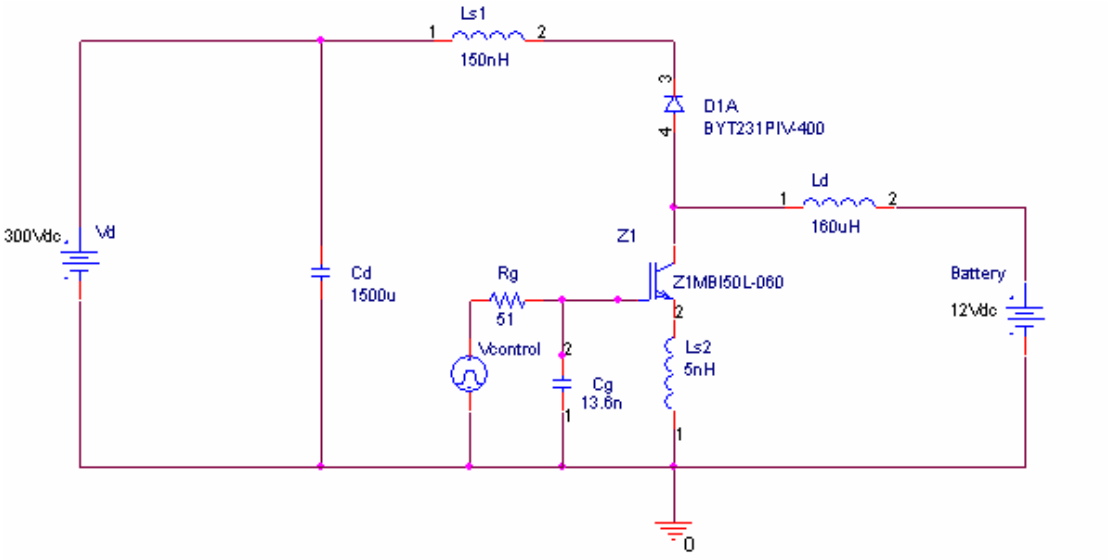

Fig 3.8 Simulation Circuit

The table below compares the parameters of the IGBT in the practical set-up and the one in the simulation set-up.

Table 3.1

	Practical (2MBI 50N-060)	**Simulation (Z1MBI 50L-060)**
Rated Voltage (V)	600	600
Rated current (A)	50	50
Typical turn-on time (µs)	0.6	0.4
Typical rise time (µs)	0.2	0.3
Typical turn-off time (µs)	0.6	0.6
Typical fall time (µs)	0.2	0.2

4.0 MEASUREMENTS

To accurately determine the switching power losses, measurements need to be taken of the switching transients during the turn on and turn off intervals. This requires accurate measurement techniques with minimum error, minimal outside interference and correct bandwidth. The main quantities to be measured are the current and voltage. Since the currents and voltages to be measured will be quite high, there is need to use measurement methods which step down the voltage and provide some form of isolation between the measurement object and the oscilloscope.

The data sheet of the IGBT to be tested shows that its rise time and fall time are a maximum of 0.6µs and 0.35µs respectively [6] which are equivalent to a high frequency content beyond 10MHz. This high frequency gives a demand on the performances of the voltage and current probes which should be carefully examined. This also means that the resonances between stray inductances and parasitic capacitances, and other phenomena usually associated with radio frequencies can significantly distort the measurements.

4.1 Voltage measurements

Voltage can be measured using a suitable voltage divider probe. For a maximum DC link voltage in the range of 300 to 400V, a suitable oscilloscope probe with a high bandwidth is found to be sufficient. For this project a Lecroy AP032 differential probe, with a bandwidth of 15MHz was used.

A differential probe is designed for applications where voltages must be measured relative to a floating voltage different from the oscilloscope ground potential. This reference voltage could be up to several hundred volts above or below ground level. Differential probes are also advantageous to use when the measurements require the rejection of common mode signals and where ground loops and currents produce excessive signal interference.

The differential probe is able to acquire the measured voltage without a ground reference, and processes it and gives out a single ended signal which can be measured by a grounded oscilloscope [7]. Fig 4.1 shows the internal circuit of the differential probe.

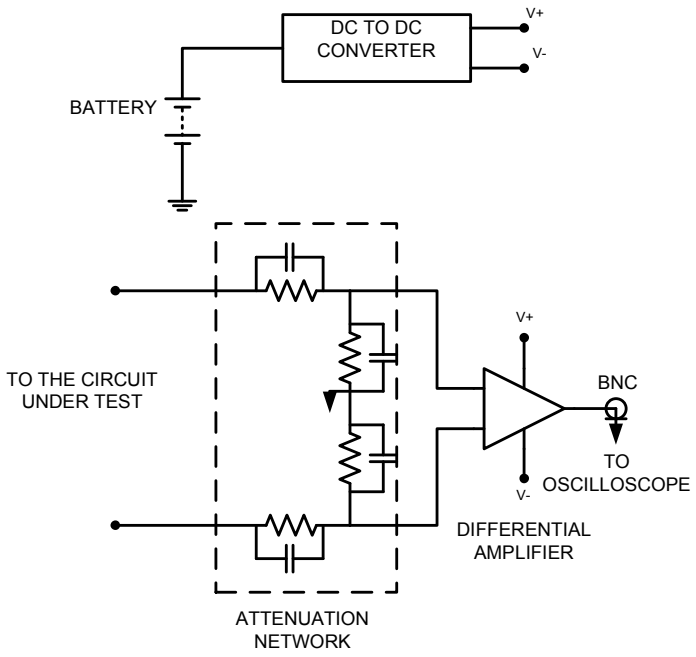

Fig 4.1 Differential probe Circuit [7]

4.2 Current Measurements

There are a number of methods that can be used for measuring current. The factors to consider when determining which method to use include suitable bandwidth, safety, ease of installation, ease of construction (if it has to be self made), and cost. Some current measurement methods which were considered for this project include co-axial shunts, current transformer, Hall Effect sensor and Rogowski coil.

The table below gives a comparison of the different current measuring methods.

Table 4.1 Comparison of current measuring Methods [8]

	Co-axial Shunt	**Current Transformer**	**Hall Effect Sensor**	**Rogowski Coil**
Isolation	None	Good	Good	Good
DC Response	Good	None	Good	None
Low Freq Response	Good	Moderate	Good	Good
High freq Response	Good	Moderate	Poor	Good
Output	Voltage	Current	Voltage	Voltage
Ease of installation	Not easy	Easy	Not easy	Easy
Ease of construction	Not easy	Easy	Not easy	Not easy
Cost	Expensive	Moderate	Cheap	Cheap

Because of its ease of construction and installation, it was decided to design and construct a current transformer with a high bandwidth.

4.3 Current Transformer Design

Fig 4.2 shows the vertical cross-section of a transformer with one primary winding and several secondary windings, wound on a bobbin. Fig 4.3 shows its equivalent circuit.

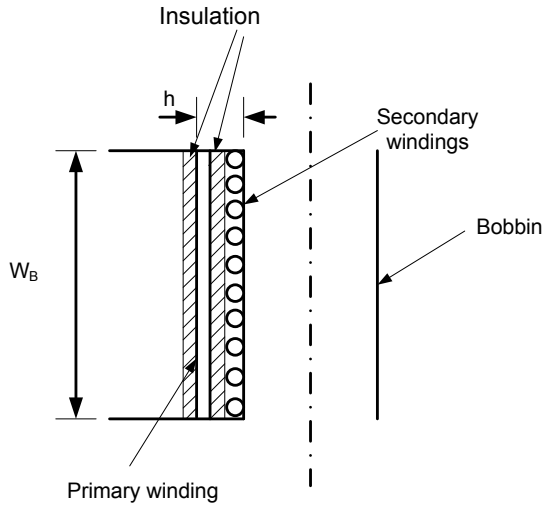

Fig 4.2 Vertical cross section of current transformer

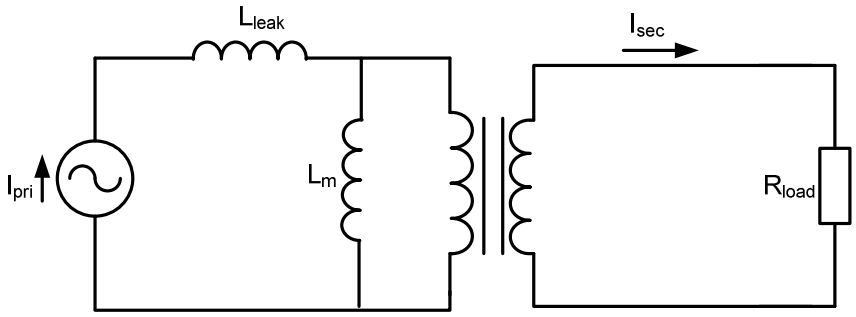

Fig 4.3 Equivalent circuit of current transformer

The leakage inductance is given by

$$L_{leakage} = \frac{\mu_0 (N)^2 h l_{av}}{3W_B}. \tag{4-1}$$

Where h and W_B are the dimensions shown in fig 1 and l_{av} is the average distance around the bobbin.

The magnetizing inductance is given by

$$L_m = \frac{N^2 A_{Fe}}{l_{Fe}} \mu_o \mu_r. \tag{4-2}$$

Where N is the number of secondary turns, A_{Fe} is the cross-sectional area of the core; l_{Fe} is the effective length of the magnetic circuit.

The time constant of the current measurement system is given by

$$T = \frac{L_m}{R_{load}}. \tag{4-3}$$

Where R is the load on the CT secondary

The voltage drop due to the CT's leakage inductance is given by

$$V_{drop} = L_{leakage} \frac{di}{dt}. \tag{4-4}$$

Where, di/dt is the rate of rise or fall of the current.

4.3.1 Design Calculations

The transformer core is a N27 ferrite and the dimensions of the CT are as follows:

W_B =38.1mm.
A_{Fe} =260mm^2.
l_{Fe} =140mm.
μ_r=1540.
l_{av} = 80mm.
h = 3mm.
N =40

Using these values in (4-1) yields the leakage inductance as seen from the primary winding as

$L_{leak\ (pri)}$ = 2.64nH.

Referred to the secondary side the leakage inductance is 4.22 µH.

Using (4-2) yields the magnetizing inductance is obtained as:

$L_{m\ (sec)}$ = 5.75mH.

Referred to the primary side the magnetizing inductance is 3.6µH.

The load resistance on the secondary side is 1Ω. Using this value in (4-3) gives the time constant as,

T = 5.75 ms.

The IGBT used in the experimental set-up (2MBI 50N-060) has a typical current rise and fall time of 0.2µs [6]. Assuming a current of 50A and using (4-4), the voltage drop is obtained as:

V_{drop} = 0.66 V

To improve its high frequency response a number of aluminium foil shields were included in its construction. One shield was between the secondary winding and the main insulation between the secondary and primary windings. The other shield covered the entire transformer core. The shields were connected together and grounded at the same point as the IGBT emitter.

Fig 4.4 shows a photo of the CT as it was connected in the set-up. Also shown in the picture are the measuring load resistors and the BNC connection to the oscilloscope.

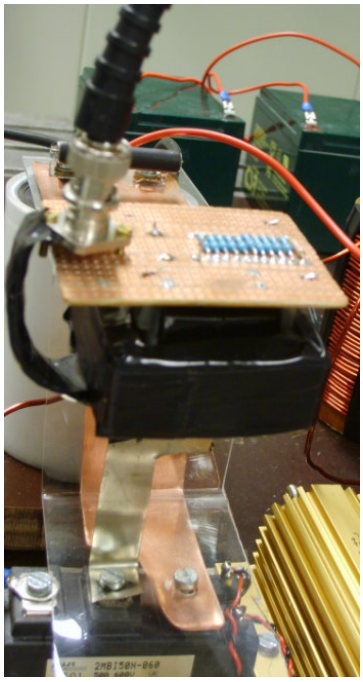

Fig 4.4 Photo of CT connected to the IGBT emitter

The CT was constructed to follow the calculated values as closely as possible, and its performance was compared to commercially available probes (Tektronix A6303 with TM504 current probe amplifier and Lecroy current probes AP011 and AP015).

4.4 Calibration of the CT

The parameters of the CT were determined experimentally and compared to the calculated values.

To determine the leakage inductance, the transformer short circuit test was used, in which a voltage was applied to the secondary winding, while the primary winding was shorted. The current through the transformer was determined by measuring the voltage drop across a resistor connected in series with the windings.

To determine the magnetizing inductance, the transformer open-circuit test was used. Here a voltage was applied to the secondary winding with the primary winding open-circuited. Current was measured as explained above.

From the measured voltages and currents, the inductances (as seen from the secondary side) and the transformation ratio were determined and they are given in table 4.2 below.

Table 4.2

Quantity	Calculated	Measured
Leakage Inductance	4.22μH (secondary)	32μH (secondary)
Magnetizing Inductance	5.74mH (secondary)	7.5mH (secondary)
Transformation ratio	40:1	41:1

It can be seen that there is a big difference in the calculated and measured values of the leakage inductance. This is because during the construction of the CT there were some deviations from the distances used in the calculations.

To measure the current through the IGBT, the CT was located on the emitter of the lower IGBT of the phase-leg module. The negative copper plate of the DC link was connected to the primary winding of the CT. To be able to compare measurements with other probes of the clip-on type, the part of the CT primary winding connected to the IGBT emitter was made narrow enough for the clip-on probes to fit. Fig 4.5 shows the location of the CT and the clip-on probe.

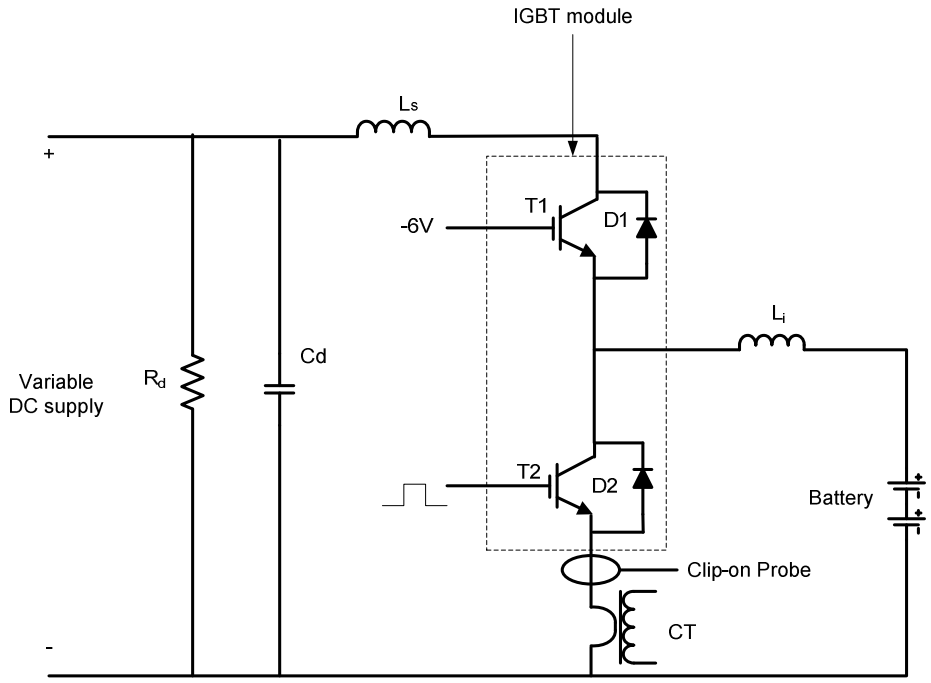

Fig 4.5 Location of CT and Clip-on probes

Fig 4.6 shows the current measured by the CT and the clip-on probe at turn-on and turn off of the IGBT.

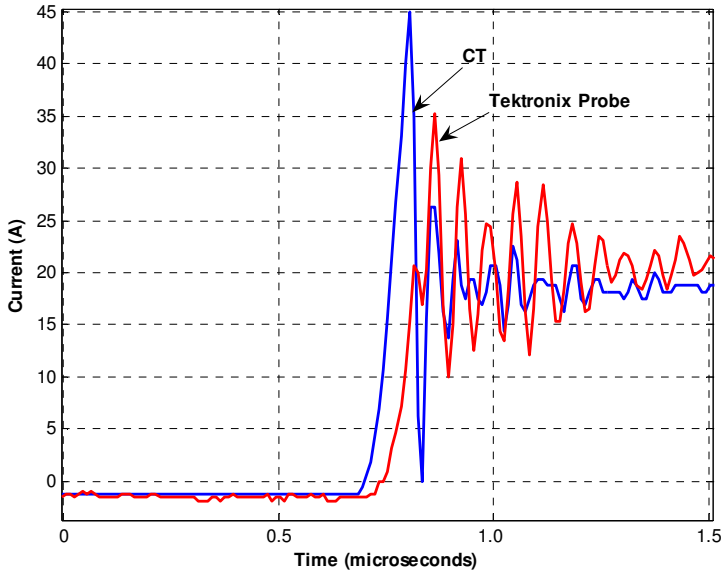

(a) Turn-on current

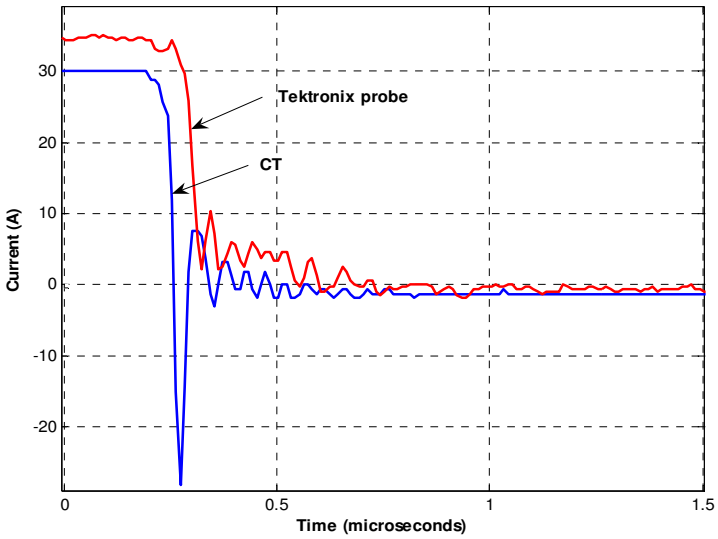

(b) Turn-off current

Fig 4.6 Currents at turn-on and turn-off measured with CT and Tektronix probe

In figs 4.6 (a) and (b), the CT current is multiplied by the number of secondary turns of the CT which is 40. However, it can be seen that this current is lower than that measured by the Tektronix probe. This shows that the CT has a magnitude error of about 14% and this need to be corrected for.

Figs 4.7 (a) and (b) show the same currents with the magnitude correction factor applied. The two currents can now be seen to have the same magnitude.

The other difference that can be seen in the two currents is in the response time. The CT is seen to respond 0.05μs before the Tektronix probe does. This is because the probe and its associated amplifier have a finite delay time.

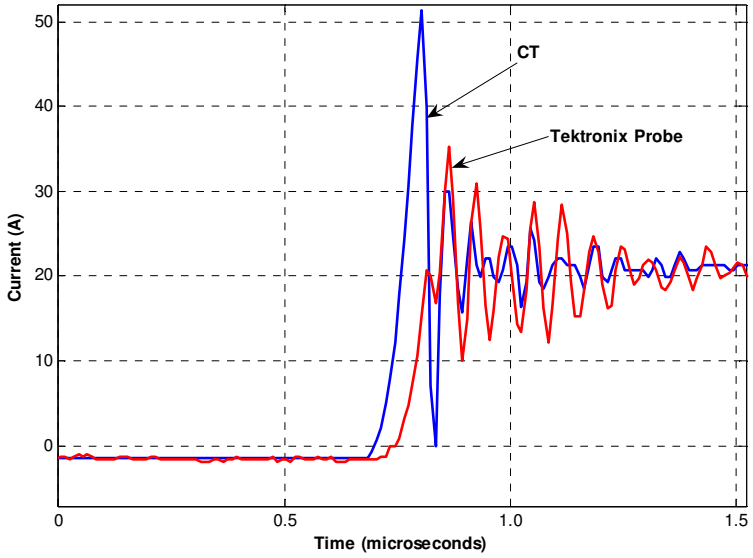

(a) Turn-on current

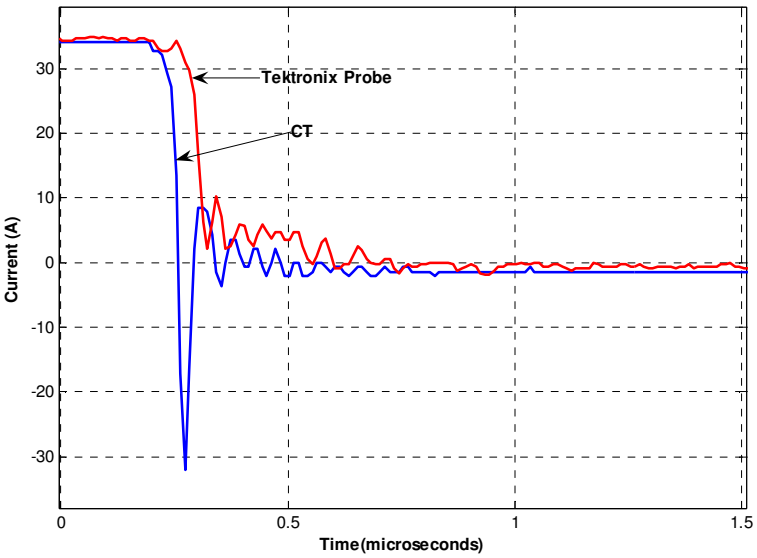

(b) Turn-off current

Fig 4.7 Currents at turn-on and turn-off with CT Magnitude Correction Factor Applied

5.0 RESULTS AND ANALYSIS

In this chapter the obtained experimental results and the energy losses computed from them are presented. Measurements and loss calculations performed under different conditions are presented. Factors which affect the switching losses include: turn-on and turn-off transient times, voltage and current level, gate resistance, oscillations, and stray inductances.

5.1 Turn on Transient

Fig 5.1 shows the turn-on transient of the IGBT. Fig 5.1(a) is taken from the practical measurements and fig 5.1(b) is from the simulation.

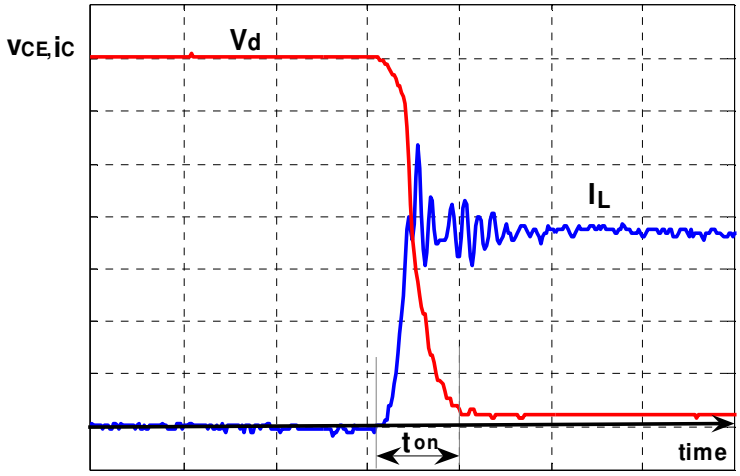

(a) Measured

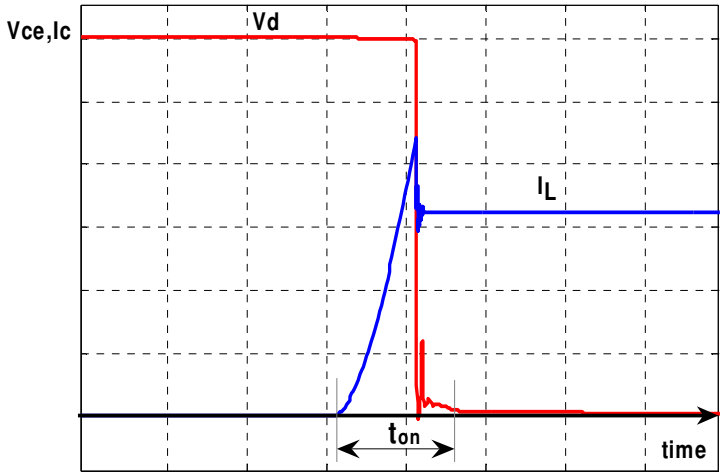

(b)Simulated

Fig 5.1 Turn-on transient (Voltage: 42.5V/div, Current: 5A/div, Time: 0.5µs/div)

From the two figures it can be seen that there are some differences in the measured and the simulated results, particularly the rise and fall times of the voltage and current. This could be due to the differences in the IGBT and diode models used in the simulation and the ones in the practical set-up and the other circuit conditions, such as the stray inductances.

5.2 Turn off Transient

The figure below shows the measured turn-off transient of the IGBT.

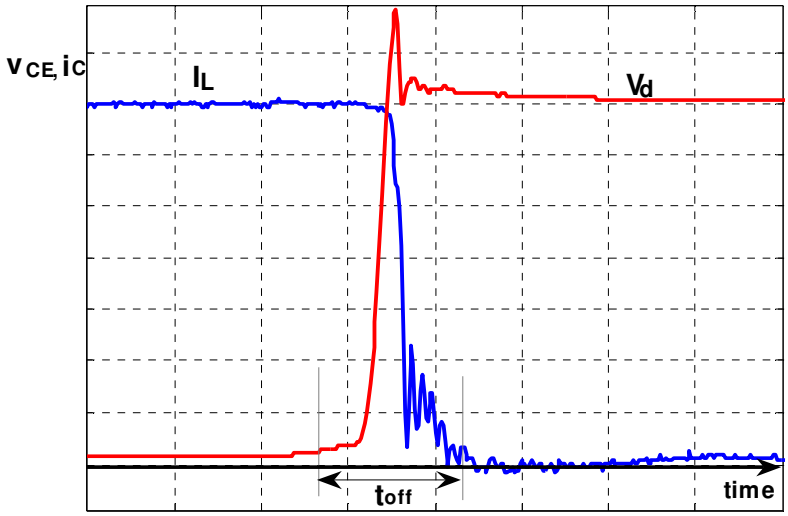

(a) Measured

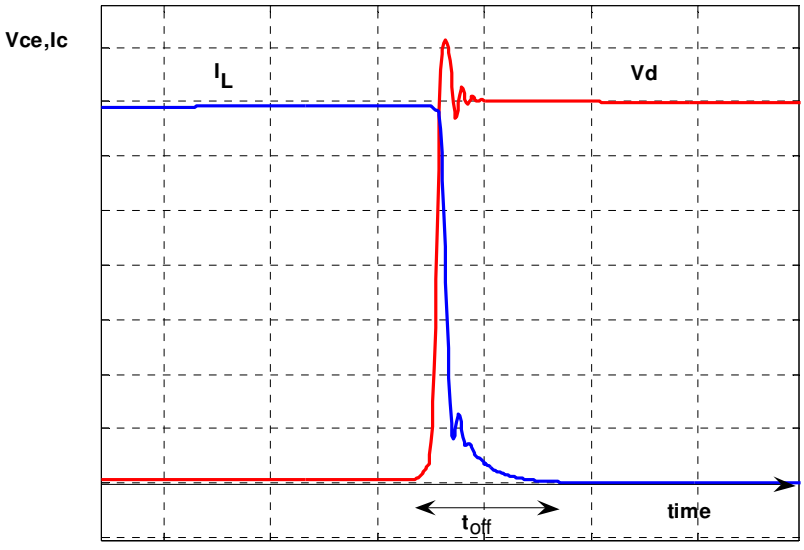

(b)Simulated

Fig 5.2 Turn-off transient (Voltage: 42.5V/div, Current: 5A/div, Time: 0.5µs/div)

As in the case for the turn-on transient, there are some differences observed in the turn-off transient due to the same reasons as the ones given earlier. One notable difference is the spike in the voltage, which in the measured curve is about 80V, while in the simulated one it is about 45V. This is due to differences in the stray inductance, and it influences the difference in the turn-off losses between the measured and the simulated cases.

The current level at turn-off is determined by the size of the inductor, the applied voltage on the load side (from the batteries) and the duration of the first control pulse.

5.3 Effect of Gate Resistance

The switching losses were measured at different voltage levels with different values of gate resistance. Four different values of gate resistance, R_g, were used, these being, 13Ω, 27 Ω, 51 Ω and 130 Ω.

5.3.1 Turn-on

Fig 5.3 shows the effect of changing gate resistance on the turn-on losses for both the measured and simulated results. The measurements were done at DC link voltages ranging from 50V to 400V.

From the measured results it can be observed that the turn-on losses tend to increase with increased gate resistance. This is because increasing the gate resistance increases the switching time. However, it can also be observed that when R_g is between 13Ω and 51 Ω, the increase is not much, but when R_g = 130 Ω, there is a remarkable increase.

From the simulation results, the effect of changing R_g is not very apparent. This is because the increase in switching time due to the increasing gate resistance is counterbalanced by a reduction in the high frequency oscillations and spikes present during the switching interval. This is illustrated in fig 5.4 for gate resistances of 13Ω and 130 Ω respectively. The figures show that for the lower gate resistance, the turn-on time is about 0.6μs while for the higher resistance it is about 1.5μs and the waveforms for the lower resistance shows a lot of oscillations and spikes. This contributed to the inaccuracy in the analysis of the simulated results.

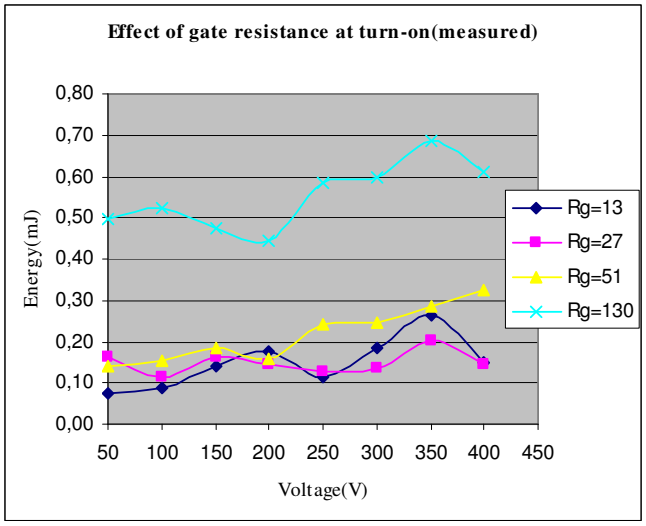

(a)Measured

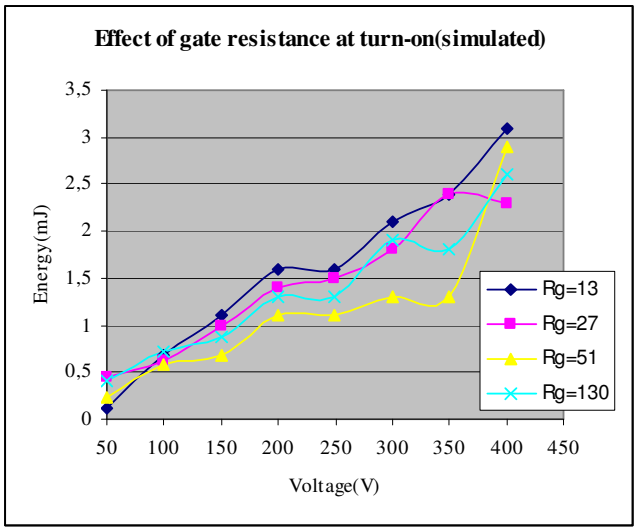

(b) Simulated

Fig 5.3 Effect of varying the gate resistance on the turn-on losses

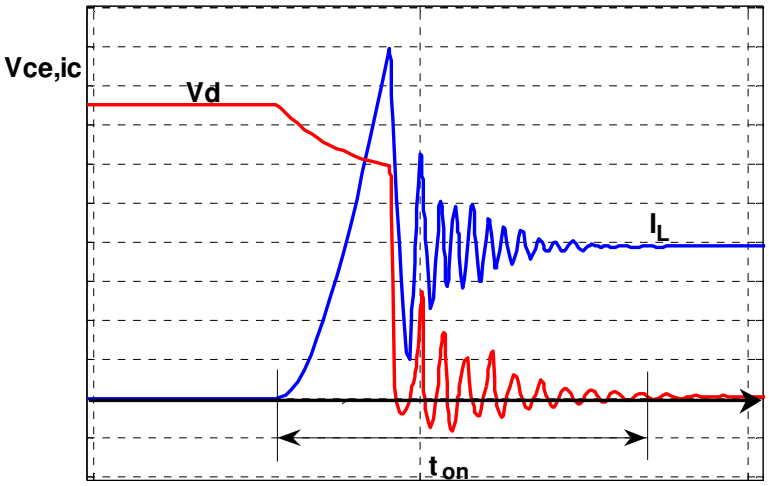

(a) Simulated turn-on with Rg=13Ω

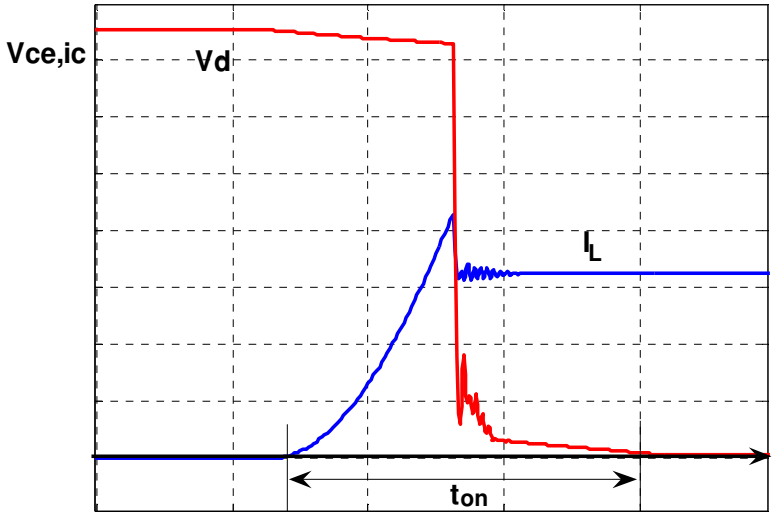

(b) Simulated turn-on with Rg=130Ω

Fig 5.4 Simulated turn-on waveforms at different values of gate resistance (Voltage: 40V/div, Current: 5A/div, Time: 0.5µs/div)

5.3.2 Turn-off

Fig 5.5 shows the effect of varying gate resistance on the turn-off losses for a DC link voltage ranging from 50V to 400V.

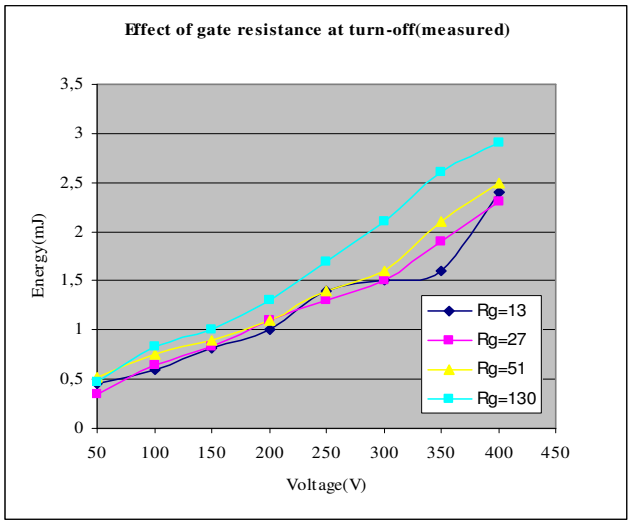

(a) Measured

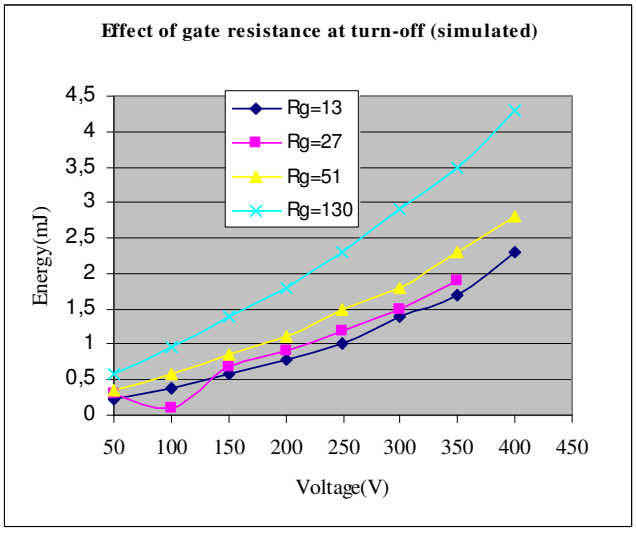

(b) Simulated

Fig 5.5 Effect of varying the gate resistance on the turn-off losses

From fig 5.5 it can be observed that the turn-off losses tend to increase with increasing gate resistance.

For the measured results, the increase is not so apparent for gate resistance ranging from 13Ω to 51Ω but for R_g = 130 Ω, the change is more apparent. The same can be said for the simulated results.

Thus it can be concluded that for the IGBT module in the practical set-up, the effect of increasing gate resistance at both turn-on and turn-off is to increase the losses, while for the IGBT model in the simulation, the effect of increasing the gate resistance on turn-on losses is not very pronounced, but at turn-off it increases the losses significantly.

5.4 Effect of Current

To determine the effect of current on the switching losses, the inductance was increased to about 230µH by connecting two inductors of 150µH and 80µH in series. The current level was varied by adjusting the first pulse width, and all measurements were done at 300V.

Fig 5.6 shows the variation of turn-on losses with current for both the measured and simulated results. It can be seen that for both the measured and the simulated result, the losses increase with the current level. The measured losses are also seen to be much lower than the simulated losses. This is because in the simulated case, the turn-on transition takes a much longer time than in the practical case. This could be due to differences in the structure of the freewheeling diode, and the IGBT such as the reverse recovery of the diode. The diode used for the simulation was rather slow compared to the practical one. This allows comparison of the effect of two diodes with different reverse recovery characteristics.

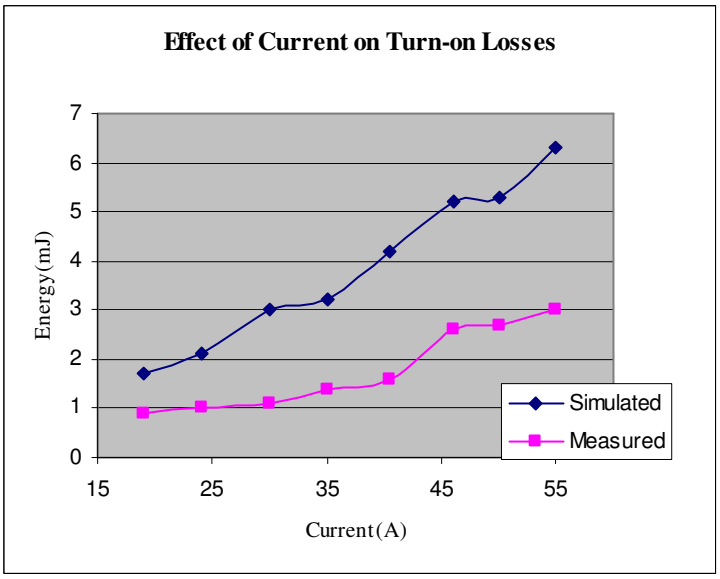

Fig 5.6 Variation of turn-on losses with current

Fig 5.7 shows the variation of turn-off losses with current. They are also seen to increase with increasing current, and the measured losses are higher than the simulated losses.

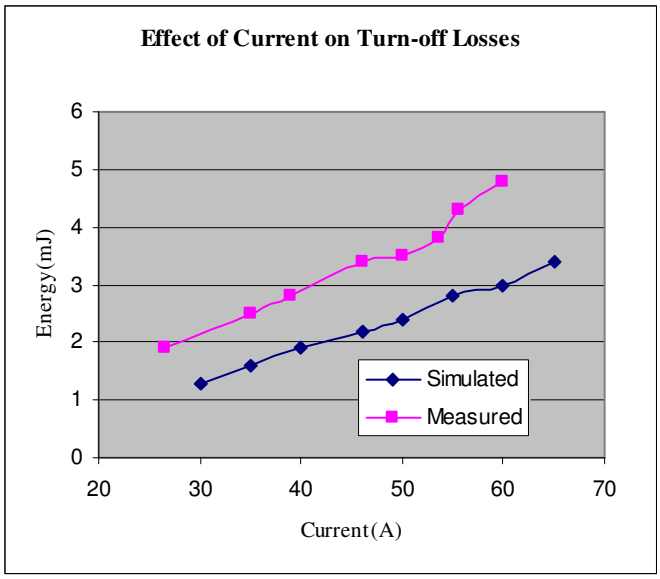

Fig 5.7 Variation of turn-off losses with current

5.5 Effect of Temperature

The effect of temperature on the measured switching losses was also investigated. The voltage was kept constant at 300V, and the current at turn-off was 60A, while at turn-on it was 45A. The temperature was increased steadily from 20˚C to 100˚C and measurements were taken at several temperatures.

Fig 5.8(a) shows the measured current and voltage at 20˚C and fig 5.8(b) shows the measured current and voltage at 100˚C. From the two figures it can be observed that the switching transition takes a longer time at 100˚C than at 20˚C.

Fig 5.9 shows the effect of temperature on the turn-on losses. The losses increase with increasing temperature because, the turn-on transition time increases.

Fig 5.10 shows the variation of turn-off losses with temperature. Here also, the losses are seen to increase with increasing temperature. It can be observed that beyond 75˚C the rate of increase of the losses with temperature is greater than at lower temperatures.

Thus, it can be concluded that increasing the temperature increases the switching losses significantly and therefore, in practical operations it is desirable to keep the temperature reasonably low to keep the switching losses low.

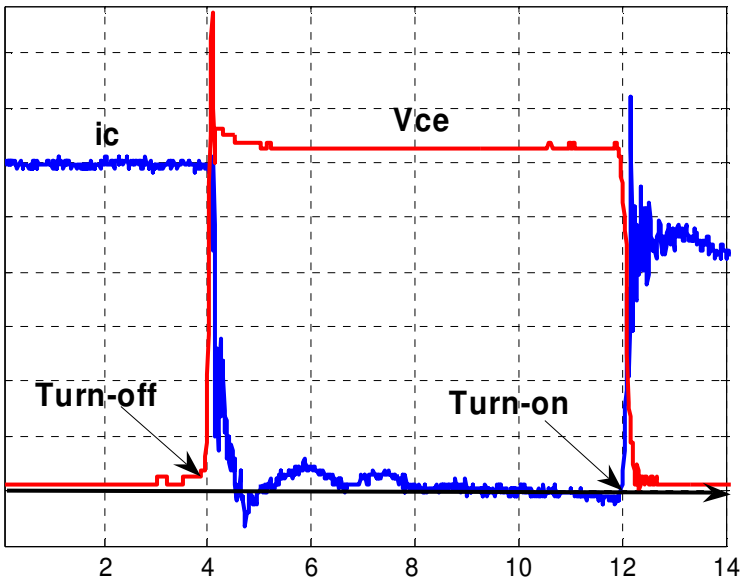

(a) Switching waveforms at 20˚C

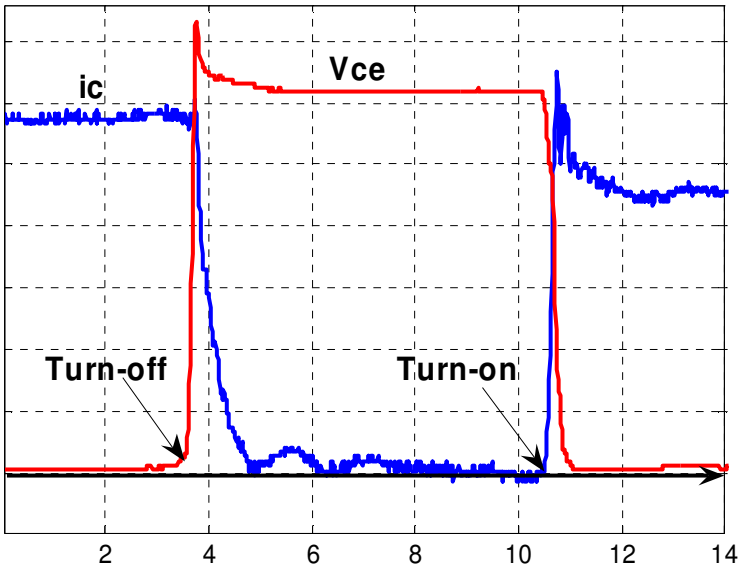

(b) Switching waveforms at 100˚C

Fig 5.8 Measured voltages and currents at different temperature (time in μs; voltage: 50V/div; current: 10A/div)

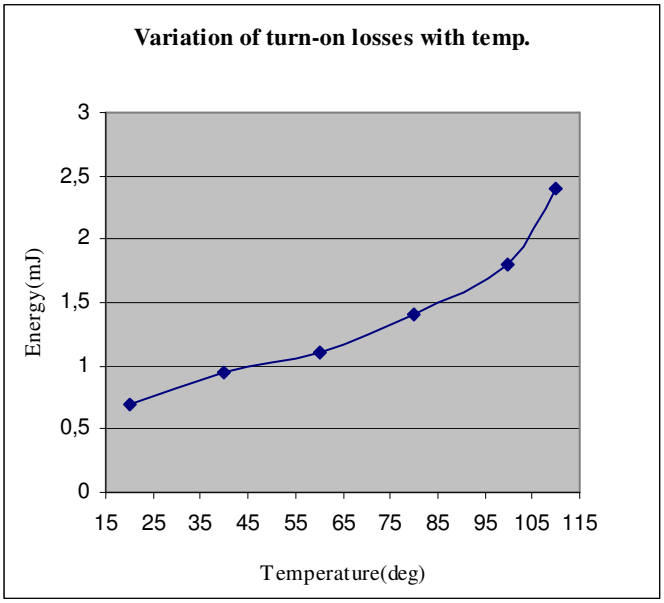

Fig 5.9 Variation of turn-on losses with temperature

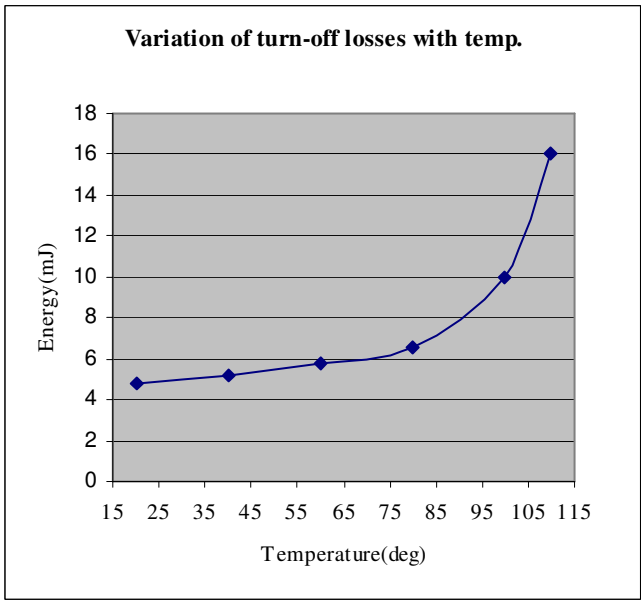

Fig 5.10 Variation of turn-off losses with temperature

6.0 CONCLUSION

The experimental setup was designed and constructed. The practical measurements in this project were performed on a half-bridge IGBT module (2MBI 50N-060) with inbuilt freewheeling diodes while simulations were done using a different, single IGBT module (Z1MBI 50L-060) with a separate freewheeling diode different from the one in the practical set-up.

From the measurements and simulations, the switching losses were determined under different conditions.

It was found that increasing the voltage and the current level increases the switching losses.

Increasing the value of the gate resistor tends to increase the switching losses. However, the effect was not very apparent for small changes but for a considerable increase in the value of the gate resistor, the change was apparent.

Another factor that was found to increase the losses was temperature, whose effect was to increase the losses as it was increased. The effect was similar for both turn-on and turn-off losses.

Other factors which could have affected the results, though they were not investigated explicitly include high frequency oscillations during the switching transition and voltage spikes caused by stray inductances.

6.1 Recommendations and Future Work

Looking at the developments in the technology and manufacture of IGBTs for high voltage and high power applications, it is necessary to expand this experimental setup be to be used for testing high voltage IGBT modules.

Currently there are IGBTs with voltage ratings of 6.5kV (e.g ABB's 5SNA0600G650100) and those with current ratings up to 1200A (5SNA 1200E330100, also from ABB).[12] and [13]. It is therefore, necessary to have a test set-up up to (or beyond) these ratings.

For security reasons, because of the high voltages involved, the set-up should be placed in a grounded metal box, with a cover. Due to the high voltage rating, the DC link capacitance can be composed of a capacitor bank with a combined voltage rating up to about 10kV. The high voltage can be supplied from a suitable high voltage DC supply (for example the *Fluke (PS) 410B*). A used one costs $995 [14]. A battery bank could be connected to supply the required high current. To give the possibility of easily adjusting the current level, a number of inductors of various sizes can be included in the design and there should be the possibility of selecting them using selector switches. The DC link

copper bars should be placed closer together, to reduce the stray inductance and a thin high dielectric strength material should be used between them.

For the current measurements, the CT can be redesigned to be able to measure the high current expected in the set-up. Alongside the CT a suitable commercial high current probe such as the *Tektronix CT4*, rated for currents up to 2.0kA and has bandwidth of 20MHz. A new one costs €3510 [15].

The voltage can be measured with a suitable high voltage, high bandwidth probe. A good choice would be the *Tektronix P6105*, rated at 40kV DC, with a bandwidth of 75MHz. A used one costs $80 on eBay [16]. Alternatively the Lecroy PPE20KV rated for 20kV with a bandwidth of 100MHz can be used. A new one costs $1695 [17] and a used one costs $995 [18].

REFERENCES

[1]. N Mohan, T.M. Undeland, W.P. Robbins, *Power Electronics, Converters, Applications and Design*, John Willey and Sons Inc, 2003

[2]. *IGBT Basics*, Application Note 9016, http://www.fairchildsemi.com/an/AN/AN-9016.pdf

[3]. K. Sheng, S.J. Finney, B.W. Williams, X.N. He, Z.M. Qian, *IGBT Switching Losses*, Proceedings IPEMC '97. Second International Power Electronics and Motion Control Conference, 1997 pt 1, p 274-7 vol 1.

[4]. *Extending the Voltage Limits of High Voltage IGBTs and Diodes,* http://library.abb.com/GLOBAL/SCOT/scot256.nsf/VerityDisplay/49F14FB55BCE6C41C1257077002B2E3C/$File/pm02mr.pdf

[5]. H.A.Wheeler, *Inductance Formulas for circular and Square Coils*. Proc. IEEE, vol.70, no.12, p1449-1450, Dec 1982.

[6] *2MBI50N-060 IGBT datasheet,* http://www.datasheetcatalog.com/datasheets_pdf/2/M/B/I/2MBI50N-060.shtml

[7].AP031/AP032 Differential Probe Operating Instructions, http://www.lecroy.com/tm/library/manuals/AP031/32/OperatorsManual/AP031_32_OM.pdf

[8]. D.A. Ward and J. La T. Exon, *Using Rogowski coils for transient current measurements,*http://ieeexplore.ieee.org/iel1/2222/5808/00222754.pdf?arnumber=222754

[9]. *Calculation of Major IGBT Operating Conditions*, Application Note ANIP9931E, http://www.infineon.com//upload/Document/cmc_upload/migrated_files/document_files/Application_Notes/anip031e.pdf

[10]. S.E.Zocholl, D.W.Smala, *Current Transformer Concepts***.** http://www.selinc.com/techpprs/6038.pdf

[11]. Muhammad. H. Rashid, *Power Electronics, Circuits, Devices, and Applications*, Prentice Hall Inc, 1993.

[12]. *IGBT Module 5SNA 0600G650100*, (Data sheet) http://library.abb.com/GLOBAL/SCOT/scot256.nsf/VerityDisplay/4CADF1D31B1BD552C12571140053E3C7/$File/5SNA%200600G650100_5SYA1558-02Jan%2006.pdf

[13]. *IGBT Module 5SNA 1200E330100*, (Data sheet)

http://library.abb.com/GLOBAL/SCOT/scot256.nsf/VerityDisplay/70BB90C34ED25DCBC1256FF50050EF85/$File/5SNA%201200E330100_5SYA1556-03May%2005.pdf

[14] *Surplus sales: Power supplies,*
http://www.surplussales.com/PowerSupplies/PowerS-8-1.html

[15] *Probes for current measurement systems,*
http://www.tek.com/site/ps/0,,51-10939-INTRO_EN,00.html

[16] *Tektronix probe prices on eBay,*
http://www.reprise.com/host/tektronix/reference/probe_prices.asp

[17] *Lecroy Price List,*
http://www.testequipmentdepot.com/lecroy/pricelist.htm

[18] *Testsmart: Probes,*
http://www.testmart.com/estore/unit.cfm/PROBES/LEC/PPE20kv/42606119/1.html

APPENDICES

Appendix A: List of Abbreviations

BJT	Bipolar Junction Transistor
CT	Current Transformer
DC	Direct Current
HVDC	High Voltage Direct Current
IC	Integrated Circuit
IGBT	Insulated Gate Bipolar Transistor
MOS	Metal Oxide Semiconductor
MOSFET	Metal Oxide Semiconductor Filed Effect Transistor
NPT	Non Punch Through
PT	Punch Through
SOA	Safe Operating Area

Appendix B: List of Symbols

Symbol	Meaning
μ_0	Permeability of free space
μ_r	Relative permeability of material
A_{Fe}	Average cross-section area of a core
BV_{CES}	Forward breakdown voltage
C_d	DC link capacitor
C_{gc}	Gate-collector capacitance
C_{ge}	Gate-emitter capacitance
C_{ies}	Gate input capacitance
d	Coil diameter
Df	Freewheeling diode
$E_{loss(off)}$	Energy loss during turn-off transient
$E_{loss(on)}$	Energy loss during turn-on transient
h	
I_C	Collector current
I_{CM}	Maximum allowable collector current
I_L	Inductor current
I_{pri}	Primary current
I_{sec}	Secondary current
l	coil length
l_{av}	Average length of a turn
l_{Fe}	Effective length of magnetic circuit
L_i	Current source inductor
L_{leak}	Leakage inductance
L_m	Magnetizing inductance
N	Number of turns
$p_{loss(off)}$	Power loss during turn-off transient
$p_{loss(on)}$	Power loss during turn-on transient
R_d	Discharge resistor
R_g	Gate resistor
R_{load}	Load resistance
T	Time constant
$t_{d(on)}$	Turn on delay time
t_{fi1}	
t_{fi2}	
t_{fv}	Voltage fall time
t_{off}	Total time for the turn-off transient
t_{on}	Total time for the turn-on transient
t_{ri}	Current rise time
V_{CE}	Collector-emitter voltage
V_d	Stiff DC voltage supply
V_{drop}	Voltage drop
V_{GE}	Gate-emitter voltage

$V_{GE(th)}$	Gate-emitter threshold voltage
V_{GG-}	
V_{GG+}	Maximum gate voltage
V_{RM}	Maximum reverse voltage
W_B	
α	Current gain of BJT

Appendix C: Circuits

C-1: Control Circuit

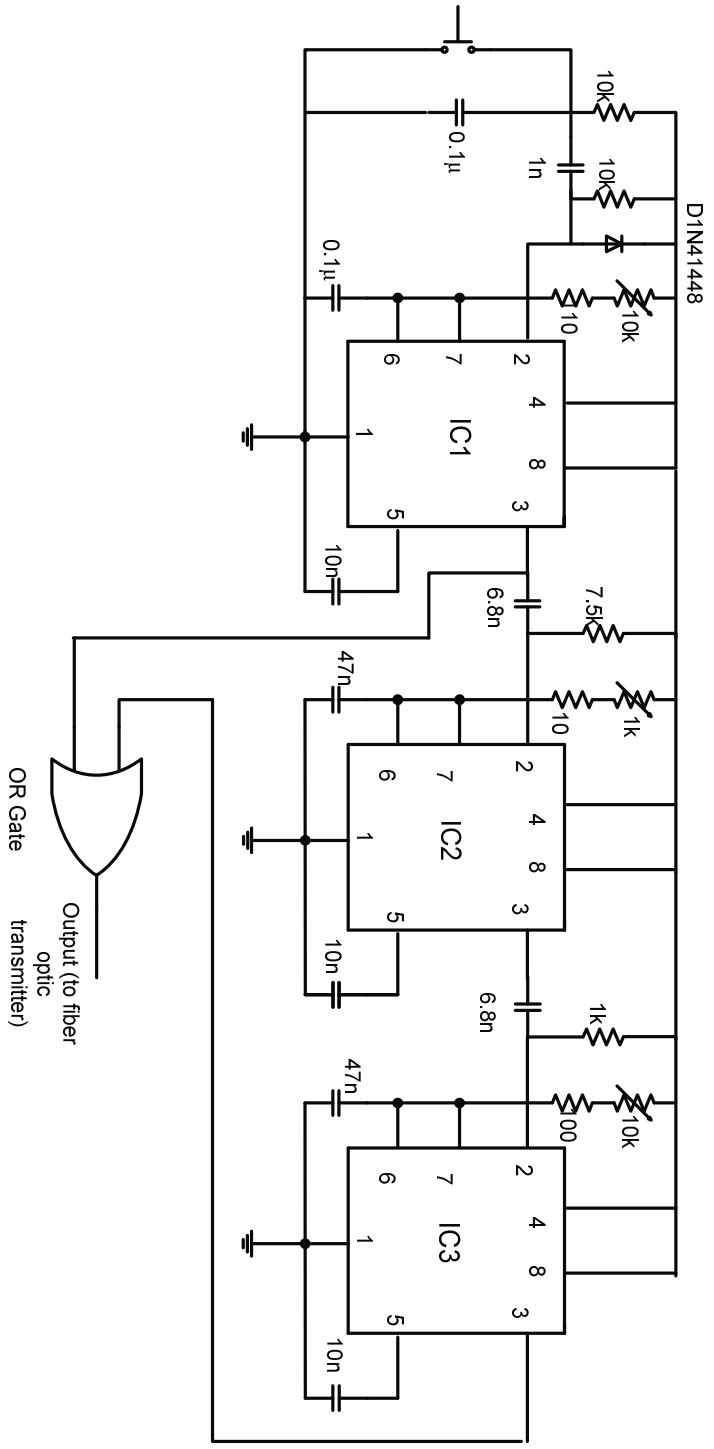

All ICs are 555 timers.

C-2: Drive Circuit

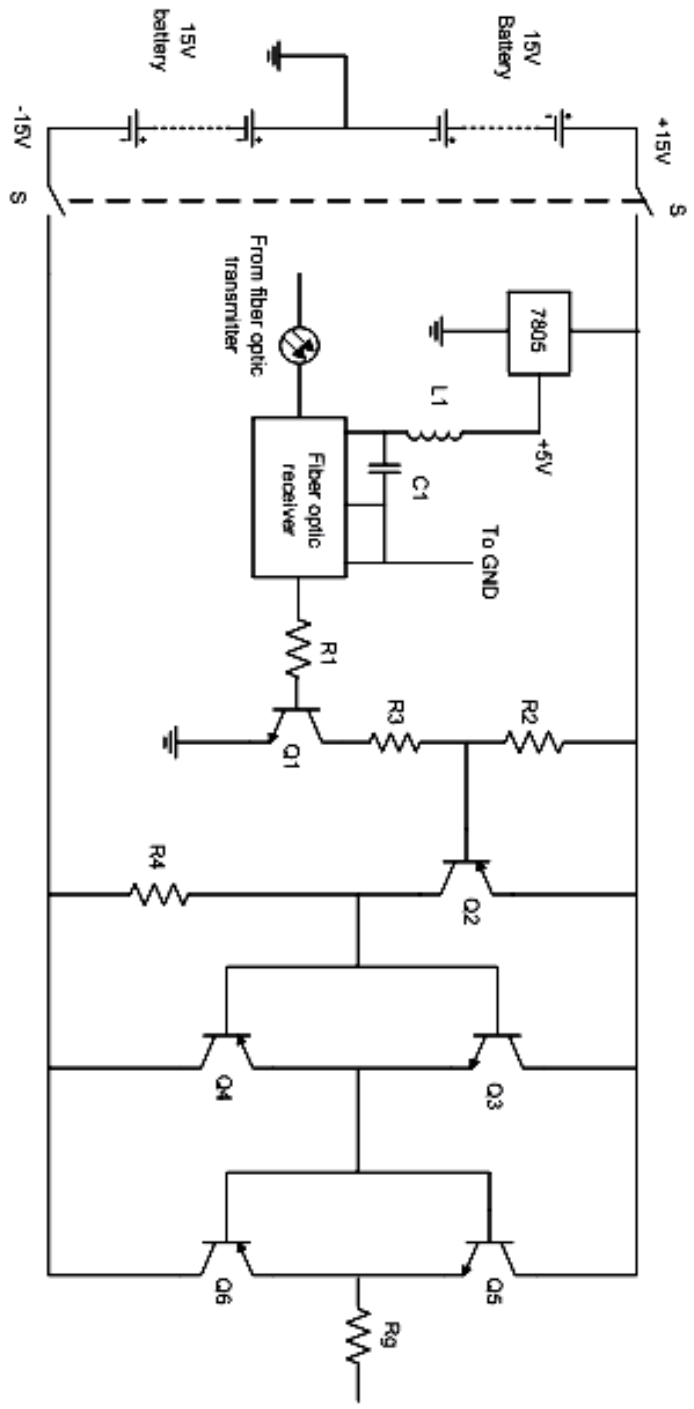

Drive Circuit Components

Component	Type
Q_1	BC337-16
Q_2	BC327-16
Q_3 and Q_5	MJE15030
Q_4 and Q_6	MJE15031
R_1	100k, ¼ watt
R_2	1k, ½ watt
R_3	10k, ½ watt
R_4	1k, 1 watt
L_1	47µH